CHEMICAL REMEDIATION OF HIGH-B.O.D. AND DARK-COLORED EFFLUENT: EXPERIMENTAL AND COMPUTATIONAL STUDIES

Eliedonna E. Cacao
Marjorie D. Hernandez
Frances Anne V. Zamora
*Ernesto J. del Rosario**
Institute of Chemistry
College of Arts and Sciences
University of the Philippines Los Baños
College, Laguna

Abstract

Melanoidin is the main color pollutant from molasses and sugar-based factories. Its remediation is hampered by the persistence of its dark color due to its polymeric structure and its recalcitrance to microbial and chemical treatments. An anionic exchange resin method was used to decolorize melanoidin, which is also an ionic color pollutant. Several anionic exchange resins (DEAE Cellulose, DEAE Sephadex, Amberlite IRA-410, Dowex 1-X8 and chitosan) were evaluated and their ability to decolorize both the natural and the synthetic melanoidin were studied. Among the five anionic exchangers examined, DEAE-Cellulose showed the best performance for melanoidin decolorization. Three of these resins (DEAE Cellulose, DEAE Sephadex and Amberlite IRA-410) were further evaluated and characterized using Hyperchem and AUTODOCK. DEAE Sephadex was observed to have the lowest docking energy and Gibbs energy of binding. Furthermore, strong oxidizers such as ozone are needed in the chemical remediation of this important pollutant. The kinetics of ozonation of synthetic glucose-glycine prepared melanoidin was studied in unbuffered and buffered solutions (pH 3.5 -10). The reaction was found to obey first-order and half-order kinetics based on absorbance data at 475 nm and 280 nm, respectively. After two hours of ozonation, melanoidin decolorization was in the range 64–94%; decolorization was greater at lower pH values. Microbial decolorization was also performed. Synthetic glucose-glycine melanoidin, after partial purification by Sephadex G-100 chromatography, was ozonated and then used as culture substrate for Bacillus subtilis. Ozone treatment for 15, 30 and 60 minutes resulted in decolorization (reduction in absorbance at 475 nm) values of 21.4 %, 41.3 % and 65.3 %, respectively; corresponding molecular weight (MW) values were 18.8, 15.3 and 9.0 kDa compared with a MW of 51.6 kDa for raw melanoidin. The pH of the melanoidin solution decreased from an initial value of 6.4 to 5.3, 4.9 and 4.6 after 15, 30 and 60 minutes of ozonation, respectively. The 1-hour ozonated melanoidin showed further 23 % decolorization after bacterial treatment for 1 – 5 days. The final MW values after combined ozonation and bacterial treatment were 16.6, 13.2 and 7.8 kDa for 15, 30 and 60 minutes ozonation, respectively. Using computational chemistry, it showed that the melanoidin structure proposed by Yaylayan and Kaminsky (1998) had the least value (most negative) of heat of formation, both in vacuo and solvated system. Thermodynamically, this is the most stable among the Cammerer-Kroh (1995) and the Kato-Tsuchida (1981) structures of melanoidin.

Keywords: color pollutant, melanoidin, Maillard reaction, bacterial decolorization, computational chemistry, ozonation, Hyperchem, AUTODOCK, docking, solvation

Introduction

Melanoidin is a major color pollutant from molasses-based fermentation plants, alcohol distilleries and sugar processing factories. It collectively refers to dark-brown, high-polymeric compounds, which is formed by a non-enzymatic browning (Maillard) reaction between a reducing sugar and an amino compound upon heating. Melanoidin is found to be negatively charged because of the dissociation of carboxylic and hydroxylic groups (O'Melia, et. al., 1978) but the detailed molecular structure has not yet been established. Formation of this polymer is very complex and can be influenced easily by the change in reaction conditions (Cämmerer and Kroh, 1995). Concentration, pH, temperature, pressure, reaction time, water activity and inhibitors are some factors affecting the Maillard reaction.

*Corresponding author

Color pollution is one of the many environmental problems that interest scientist nowadays. High biochemical oxygen demand (BOD) and dark-colored effluents, especially melanoidin-containing wastewater from alcohol distilleries provide serious challenges for waste treatment. Several studies have been conducted to obtain knowledge about melanoidin. However, more research and development (R & D) studies are needed in order to evaluate various promising methods for BOD reduction and decolorization of problematic effluents like melanoidin.

Decolorization and Degradation of Melanoidin

Due to the characteristic dark color of melanoidin, which contributes to color pollution, decolorization and degradation of this polymer is a necessity. Through the years, color removal and degradation of melanoidin involving microbial and chemical treatment has been the goal of several researches.

Several fungi and bacterial species have been found effective in decolorizing molasses wastewater. Strains of *Basidomycetes* (Hongo *et al.*, 1973) were found to be good decolorizing agents under highly aerated systems, while *Coroilus* Ps4a (Tozawa *et al.*, 1979) decolorized molasses (10%) from fermentation liquor at 30°C after 5 days of incubation. Paje (1987) observed that addition of glucose favored growth of the fungi and decolorization of the media.

Magbanua and coworkers (1992) decolorized alcohol distillery biodigester effluent (ADBE) using two isolates of *Bacillus subtilis* immobilized in alginate gel beads. A relative color removal (RCR) value of 75% was obtained for ten-fold diluted effluent while a lower RCR was obtained at lower dilution. The same authors conducted screening for 236 filamentous fungi and found that 12 isolates gave more than 40% RCR of ADBE at five-fold dilution. Two fungal isolates of *Aspergillus* (MD-1 and MD-2) were further tested for their ability to decolorize Melanoidin Pigment Broth (MPB). Preliminary results indicated that these isolates have higher capability of decolorizing melanoidin than those observed for immobilized bacteria. Like bacteria, these two isolates could decolorize pure melanoidin although color reversal was observed for isolate MD-1 due to unknown cause. Another observation noted was the rapid growth and large production of mycelia of these two isolates in MPB.

Rico (1996) who studied changes in some molecular properties of synthetic and natural melanoidin after decolorization by *Bacillus subtilis* obtained 71.87% and 61% decolorization of synthetic and natural melanoidins, respectively, with an inoculum size of 1.7×10^9 cfu/mL under optimal conditions after 8 days of fermentation. Parameters such as MW, intrinsic viscosity, UV-Vis and IR spectra were examined. A decrease in average MW and intrinsic viscosity was observed for both synthetic melanoidin and natural melanoidins. The UV-Vis spectra showed increase in absorbance at 220-380 nm and a decrease at >380 nm after decolorization for both synthetic and natural samples. The IR spectra of the microbially treated synthetic melanoidin revealed reduced intensity of C=O and C=C absorption attributed to the alkoxy (C-O) functional group. These results indicated that the microorganism secreted an oxidase enzyme, which caused the oxidative degradation of both melanoidin samples.

Pacaliwagan (1997) performed the same set of experiments as Rico (1996) but used *Aspergillus* sp. rather than *Bacillus* sp. The fungal isolate decolorized 59.41% of synthetic melanoidin and 71.23% of natural melanoidin. The same trend was obtained for the average MW, intrinsic viscosity and UV-Vis spectrum; however the IR spectrum showed enhanced C=O and C=C absorption for synthetic melanoidin but was not determined for the natural melanoidin.

Hayase and coworkers (1984) initially used glucose oxidase to decolorize melanoidin using glucose as a substrate. Enzymatic oxidation of glucose into gluconic acid causes the production of oxidizing agents like H_2O_2. Hydrogen peroxide reacts with hydroxyl ion to perform perhydoxyl anion (HOO^-) that is a nucleophile. Under alkaline condition, there is an abundance of perhydroxyl anion, which attacks the carbonyl group in melanoidin causing decolorization and degradation of the polymer. At pH 10 (37°C), 97% decolorization of the polymer was obtained.

Del Rosario and coworkers who study the decolorization of molasses melanoidin in ADBE using ferric chloride/aluminum chloride as inorganic flocculants found that the optimum concentration of Fe^{3+} or Al^{3+} needed for decolorization was approximately 0.035M where 93% decolorization for undiluted ADBE occurred, while reduction in total organic carbon in the supernatant solution was approximately 76%. Addition to ADBE of the optimum concentration of the commercial flocculant "Polytetsu" with chemical formula $[Fe(OH)_n(SO_4)_{3-n/2}]_m$ corresponding to 0.039M Fe^{3+} in the final solution, resulted in more than 98% decolorization of ADBE and more than 90% reduction of total organic carbon in the supernatant solution.

Nondializable melanoidin prepared from a glucose-glycine system was investigated in terms of decolorization and degradation upon ozone treatment. MDA values of 84% and 97% were obtained after ozonolysis at −1°C for 10 minutes and 90 minutes, respectively. The average MW of melanoidin decreased from 7000 to 3000 Da after ozonolysis for 40 minutes. From the IR results and the finding that glycine was the major degradation product in the aqueous fraction, it was postulated that a significant amount of glycine was incorporated into the melanoidin in the amide form (Kim *et al.*, 1984)

In 1998, Amarante observed a 16% COD (chemical oxygen demand) reduction after ozonation of distillery slops for 10 hours and 28% increase in BOD. Dallo (1998) obtained a decolorization efficiency of 80% after 43 hours of ozonation of distillery slops with a corresponding decrease in pH from 4.8 to 3.7 due to formation of acids and oxidation products.

Computational Chemistry

In order to obtain more precise structural information on the reaction, computational method can be applied. The method, a sub field of theoretical chemistry is generically called computational chemistry. As generally defined computational chemistry is the area of chemistry that involves the use of computational methods in solving chemical problems. The method involves mainly the application of theories, rather than the formulation of new ones.

Computational method can be based on both quantum and molecular mechanics. Quantum mechanical calculation is based on quantum mechanical theory and starts with the premise that every chemistry is bounded to Schroedinger's equation $\mathbf{H\Psi = E\Psi}$ If a calculation is done without reference to experimental data, the method is termed as *ab initio* meaning "from the beginning." It is a more rigorous calculation compared to semi-empirical calculations. A semi-empirical method reduces calculation cost (i.e., computer time) by reducing the number of integral and some modifications with respect to experimental observations.

Molecular mechanical method, also termed as Force Field Method, greatly differs from quantum mechanical approaches in most aspects. Calculations using molecular mechanics are based on properties such as bond lengths (i.e. C-H bonds are nearly constant in all molecules), atom types and others. Moreover, calculation is relatively faster than *ab initio* method. Semi-empirical method or molecular mechanics is usually used in calculations dealing with large molecules.

A charged molecule binds to an ion exchange resin by electrostatic forces between the ligand's surface charges and the dense clusters of charged groups on the resin. The ligands displace the counter ions and become attached; generally the net charge on the protein should be the same as that of the counter ion displaced (Scopes, 1987). This principle of ion exchange is similar to docking. In any docking scheme, the ideal procedure is to find the global minimum in the potential energy surface representing the interaction between the ligand and the receptor.

Another important challenge for molecular modeling is the reliability of docking of ligand to its target. AUTODOCK software was proven to be effective in selecting correct complexes based on energy without prior knowledge of the binding site (Hetenyi and van der Spoel, 2002). This application is called blind docking.

This project involved experimental and computational studies in order to optimize and evaluate promising methods for BOD reduction and decolorization; these include adsorption, enzymatic decolorization and chemical oxidation using ozone. In addition to laboratory experiments, computer-based calculations and modeling was done in order to provide quantitative explanation for the results in terms of physico-chemical concepts.

The objectives of the study are as follows:

(1) conduct experimental and computational studies on adsorption decolorization of melanoidin (synthetic and natural) using suitable adsorbent materials;
(2) conduct experimental and computational studies on enzymatic decolorization of melanoidin using microbial enzymes; and
(3) conduct computer calculations and modeling of melanoidin decolorization by ozonation.

Materials and Methods

Experimental Part

- Sample Preparation and Purification

Synthetic melanoidin was prepared by evenly mixing glucose and glycine, both analytical grade (Ajax Chemicals) in a clean screw-capped test tube at 1:1 molar ratio. The reactants were allowed to react for 2 minutes at 160°C. The product was dissolved in a minimum amount of deionized water and was dialyzed for 24 hours using cellulosic membrane (average diameter = 16 mm) with a molecular weight cut-off of 12 kDa (Sigma Chemical Co.).

A solution of the dialyzed solvent-free initial Maillard product reaction product was eluted from a Sephadex G-75 column with phosphate buffer (0.005M) of pH 7. Fractions (4.2 ml per fraction) were collected using a BIO-RAD 2110 fraction collector and these were subjected to UV-VIS analysis using a Beckman model DU 640 Spectrophotometer. Samples were pooled on the basis of their absorbance at 280 nm and then freeze-dried.

- Molecular Weight Determination

The molecular weight (MW) of the sample was determined by gel filtration chromatography using a Sephadex G-75 column. This column was calibrated using proteins of known MW values. Fractions were collected and subjected to UV-VIS analysis.

- Quantification of Dialyzed Melanoidin

The concentration of melanoidin was determined using a Beer's Law plot. Several concentrations of dialyzed melanoidin were prepared in order to construct a calibration curve. A separate 1 ml dialyzed sample was freeze-dried in order to determine the concentration in g/ml of melanoidin.

- Anion Exchange Chromatography

The purified glucose-glycine melanoidin product mixture was eluted from a chromatographic column using one of the following exchange resins: DOWEX 1-X8, Amberlite IRA-410, DEAE-Sephadex and DEAE-Cellulose. The NaCl salt gradient concentration (using 0, 0.025, 0.05, 0.5, 1.0 and 1.5M) and the pH of the phosphate buffer (pH 6, 7 and 8) were optimized. The eluate was subjected to UV-VIS analysis at 280 nm and 475 nm. The pooled fractions were mixed and subjected again to UV-VIS analysis in order to determine the ion exchange capacity of melanoidin.

Several known salt solutions (0, 0.0001, 0.01, 0.5, 0.6, 0.7, 0.8, 0.9, 1.0, 1.5 and 2.0M) were prepared, their electrolytic conductance determined and then a calibration plot was constructed (in terms of conductance vs. concentration). The salt concentration of each collected fraction was determined by interpolation from this plot.

The effect of the buffer pH on melanoidin elution was also determined using natural melanoidin.

- Viscosity Measurements

A sample of freeze-dried melanoidin approximately 0.20g was weighed and dissolved in deionized water. Twenty-five mL dilutions were prepared from that stock solution in order to prepare the following: 8.2×10^{-5}, 2.0×10^{-4}, 5.1×10^{-4}, 1.3×10^{-3}, 3.2×10^{-3} and 8.0×10^{-3}g/ml.

Determination of flow times using an Ubbelohde viscometer was performed for the pure solvent and for the different solutions at 30 °C.

- Ozonolysis

The purified melanoidin was placed in a specially made glass reaction vessel. Glass wool was used to hold the melanoidin; ozone produced from the ozonator (Sander Ozonizer, Japan) was channeled through a glass wool filter in order to remove particulates. The ozonized melanoidin underwent the same set of analyses as that of the untreated melanoidin.

- Determination of the kinetic parameters of ozonation reaction

Determination of the kinetics of the reaction between ozone and melanoidin was carried out by keeping the concentration of ozone constant while varying the initial concentration of melanoidin. Varying concentrations of glucose-glycine melanoidin were treated with ozone for ten minutes; samples were drawn from the reaction solution at selected time intervals and the absorbance was determined at 280 and 475 nm. Initial rates of the reaction were determined by obtaining the slope of the linear portion of the curve. Equation 4 was used in order to establish the kinetic order with respect to melanoidin.

Three-milliliter aliquots were drawn from each reaction above at different time intervals (0, 0.5, 1.0, 1.5, 2.0, 2.5, 3.0, 3.5, 4.0, 5.0 and 10.0 minutes). The samples were subjected to UV-Vis analysis at 475 nm.

A plot of absorbance at 475 nm against time during decolorization of melanoidin was prepared. The rate was calculated from the slope of the tangent to the curve.

The reaction rate was measured at the beginning of the reaction for several different initial concentrations of reactants.

A plot of $M^{(1-n)}$ against t should be a straight line with slope - (1-n) k'. From the slope, the rate constant may be calculated once the order of reaction (n) has been determined.

The time course of the absorbance at 475 nm during decolorization of melanoidin by ozonolysis at different pH was observed.

Initial rates were also determined for different initial concentrations of melanoidin. A plot of the logarithm of the initial slope against the logarithm of melanoidin concentration gave a slope which corresponds to the order of the reaction. The kinetic order with respect to ozone was not determined.

➢ Microorganisms

A local isolate of *Bacillus subtilis*-Biotech 1305, obtained from the Microbial Culture Collection of BIOTECH-UPLB was used to decolorize synthetic melanoidin. The microbial isolate was maintained in Tryptone-Glucose-Yeast Extract Agar (TGYA) slant cultures and was stored at 4°C prior to use.

➢ Microbial Build-up and Course

Bacterial cells were produced using the medium which consisted of 1% glucose, 0.5% peptone, 0.3 % beef extract, 0.1% KH_2PO_4 and 0.05% $MgSO_4 \bullet 7H_2O$. The medium was first dissolved using 0.2 M phosphate buffer. The pH was then adjusted to 7.0.

Ten 250-mL Erlenmeyer flasks containing 100 ml of the medium was inoculated with the inocula from a 24-hour slant culture. The samples were shaken at room temperature (28-31 °C) for 24 hours. The cell was collected by centrifugation at 3500 rpm for 10 minutes. The microbial count was determined using the serial dilution/spread plate method.

➢ Microbial Decolorization of Ozonated Melanoidin

Both ozonated and non-ozonated melanoidin was diluted three-fold by adding 0.2M phosphate buffer (pH 7) and then the same nutrients were added as was done to prepare the bacterial medium (to final concentration). The pH was then adjusted to 7.0.

Eight 250-mL Erlenmeyer flasks were filled with 40 mL of the above-mentioned synthethic melanoidin solution. This involved the stock solution (1mg/ml), and 15min, 30min and 60min ozonated melanoidin. Four of the flasks were inoculated with 10 mL each of the cell suspension (designated as BAC-stock-15min-30min and –60min respectively). Ten mL of the sterile medium was added to each of the remaining flasks (designated as CTRL-stock-15min-30min and –60min respectively) and served as the controls. The flasks were shaken at room temperature for 5 days. One mL aliquot was obtained aseptically from each flask every 24 hours. The supernatant was analyzed in terms of percent decolorization using the reduction of absorbance at 475 nm (Migo *et. al.*, 1993) and pH.

Computational Part

Calculations were performed using HyperChem version 7.0 (Hypercube Inc., Ontario, Canada) installed in Pentium III and IV computers. The geometry of the compounds was initially optimized by molecular mechanics or semi-empirical method. The semi-empirical method used was Parametric Method 3 (PM3). Once the geometry was optimized, a PM3 single point calculation (with SCF control set to 0.01 as convergence limit and 110 as iteration limit) was performed in order to calculate molecular properties. The HOMO and LUMO energies were calculated after the single point calculation.

➢ Determination of Chemical Pathways and Mechanism for Melanoidin

Different structures of ozone were subjected to geometry optimization and calculations in order to determine the most probable and stable structure that reacts with melanoidin during ozonation. PM3 was used for the geometry oprtimization and evaluation of thermodynamically stable intermediates and reaction products of ozonation based on the Yaylayan and Kaminsky (Y-K) (1998), Cammerer-Kroh (C-K) (1995) and Kato-Tsuchida (K-T) (1981) mechanisms.

Geometry optimization using the PM3 computational method was also used for the following compounds: melanoidin, molozonide, ozonide and intermediate reaction products (based on both Y-K, C-K and K-T structures). The heats of formation of melanoidin (kcal/g) were computed and compared. Orbital calculations were also employed in order to generate molecular orbital or electrostatic potential plots. The molecular (MO) coefficients were also calculated in order to evaluate where new bonds are likely to form.

- Effect of solvent molecules in ozonation

Using HYPERCHEM, the three proposed structures of melanoidin (Cammerer and Kroh, 1995; Kato and Tsuchida. 1981; Yaylayan and Kaminsky, 1998) for different model systems in solution were evaluated. HYPERCHEM uses the TIP3P (three-point transferable intermolecular potentials) water model for solvation, which applies the Jorgensen's Monte Carlo equilibrated box of 216 water molecules. The physical properties and potential energy surfaces of molecules were computed using the classical equations in mechanics (Molecular Mechanics). Using neutral glycine as the solute, the force fields namely MM+, AMBER, BIO+CHARM and OPLS were evaluated in order to arrive at the most appropriate force field for solvated systems. The effect of increasing number of water molecules on the heat formation was also done. The heat of solvation of the structures of melanoidin was also computed.

- Binding Mode of Melanoidin to Anionic Exchangers

HYPERCHEM

Three anionic exchange resins namely DEAE Cellulose, DEAE Sephadex and Amberlite IRA-410 were evaluated and characterized. Resin properties were optimized using the molecular mechanics force field AMBER. The properties were further calculated using the semi-empirical PM3 method.

The Yaylayan-Kaminsky (1998) structure of the glucose-glycine model system of melanoidin was used as model for ligand binding to the anionic exchange resin. HYPERCHEM was used in docking melanoidin on the resin.

AUTODOCK

AUTODOCK software was also used in order to further evaluate the binding of melanoidin to the three resins used above. HYPERCHEM was used to optimize the models using AMBER and PM3 calculations. Partial charges of melanoidin were added via AUTODOCK Tools (ADT), which was also used to manipulate the model resins and melanoidin. Polar hydrogens were added to the resins. For the ligands, rigid root was defined automatically and non-polar hydrogens were merged. Solvation parameters for the resins were also adjusted.

Mass-centered grid maps were generated with 0.55 Å spacing by the AUTOGRID program. Genetic Algorithm (GA) was used for the docking of the anionic resins and melanoidin. The default docking parameters for GA (Hetenyi and van der Spoel, 2002) was used. The lowest docking energy, E_{docked}, and Gibbs free energy, $\Delta G_{binding,}$ values calculated for each melanoidin-resin complex were chosen for active site identification. Determination of the bond distances of the complex was done using Visual Molecular Display (VMD).

Results and Discussion

Anion Exchange Chromatography

The Maillard product produced after 2 minutes of heating at 160°C from an equimolar (1:1) mixture of glucose and glycine was purified by dialysis against deionized water and then eluted from Sephadex G-75 column buffered at pH 7. The elution profile of the sample is given in Figure 1.

Figure 1. Elution profile of the Maillard reaction product at 160°C on Sephadex G-75.

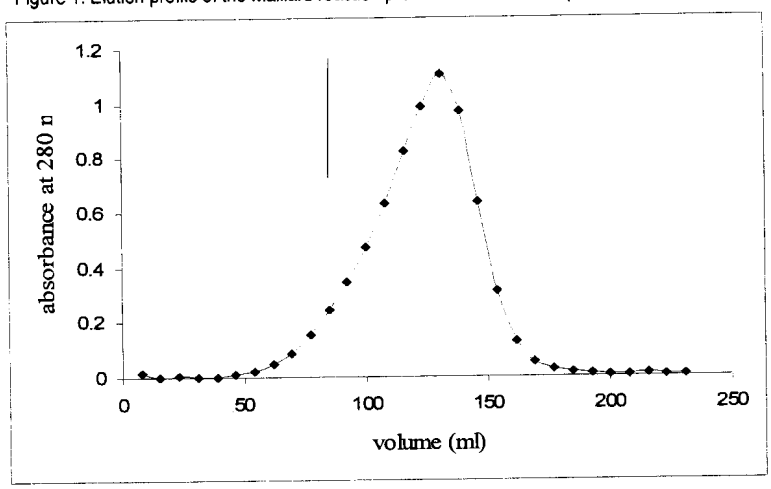

Prior to sample elution, the column was calibrated with proteins of known MW (Figure 2). Five MW standards were used: α-amylase (MW =200 000 Da), alcohol dehydrogenase (MW =150 000 Da), bovine serum albumin (MW =66 000 Da), carbonic anhydrase (MW =29 000 Da) and cytochrome c (MW =12 400 Da). Using linear correlation involving the logarithm of the standards used and the ratio of the sample volume to the void volume (V_o), the MW of the purified sample was found to be equal to 60.7 Da (average of three trials). This value is quite large compared to that (11.a kDa) observed by Escosia (2001). This only confirms that the melanoidin MW increases with reaction time (since Escosia had a one-minute reaction time while the present study involved a two-minute reaction).

Figure 2. Elution profile of the MW markers for the determination of melanoidin MW:
(A) blue dextran; (B) α -amylase; (C) alcohol dehydrogenase; (D) bovine serum albumin;
(E) carbonic anhydrase; and (F) cytochrome c.

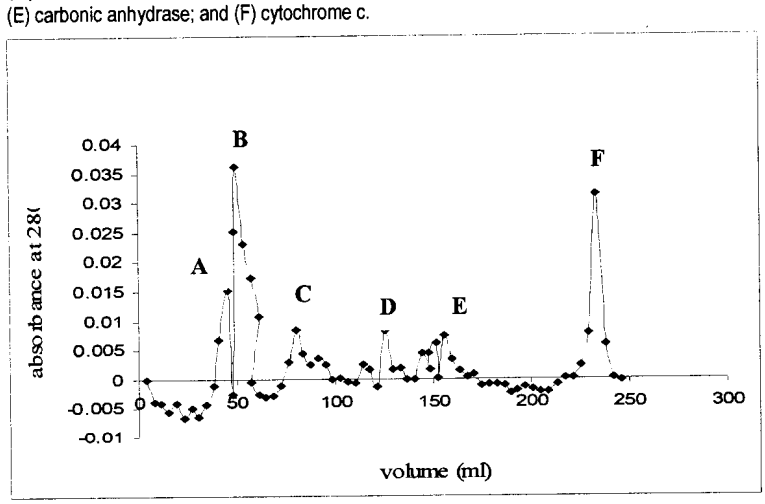

Two chloride-form resins, namely DOWEX 1-X8 and IRA-410, were capable of decolorization (although DOWEX 1-X8 showed poorer performance); unfortunately, not all of the melanoidin sample was adsorbed on the resin. There was some brown colored solution which was eluted at the void volume (see Table 1 below).

Table 1. Summary of the recovery of melanoidin sample using IRA-410 resin at different salt gradient concentrations.

Total Salt Gradient Conc. (M)	% Recovery		
	V_o	V_e remaining	$V_o + V_e$ remaining
0.5	2.27	59.76	62.01
1.0	4.19	67.47	71.66
1.5	2.84	61.45	64.29

DOWEX 1-X8 is a strongly basic anionic resin with Cl^- as its usual ionic form. Melanoidin binds to ion exchangers by electrostatic forces between the surface of negative charges and the dense clusters of charged groups on the exchangers. The melanoidin then displaces the chloride ion in the adsorbent binding site. In this resin, it can be seen (Figure 3) that at all salt gradient concentrations, the highest elution peak was observed at void volume, V_o (~22ml). With these results, one can see that there was no effective attraction between the resin and the melanoidin.

Figure 3. Elution profile of melanoidin using (a) DOWEX 1-X8 and (b) Amberlite IRA-410 at different salt gradient (NaCl) concentration.

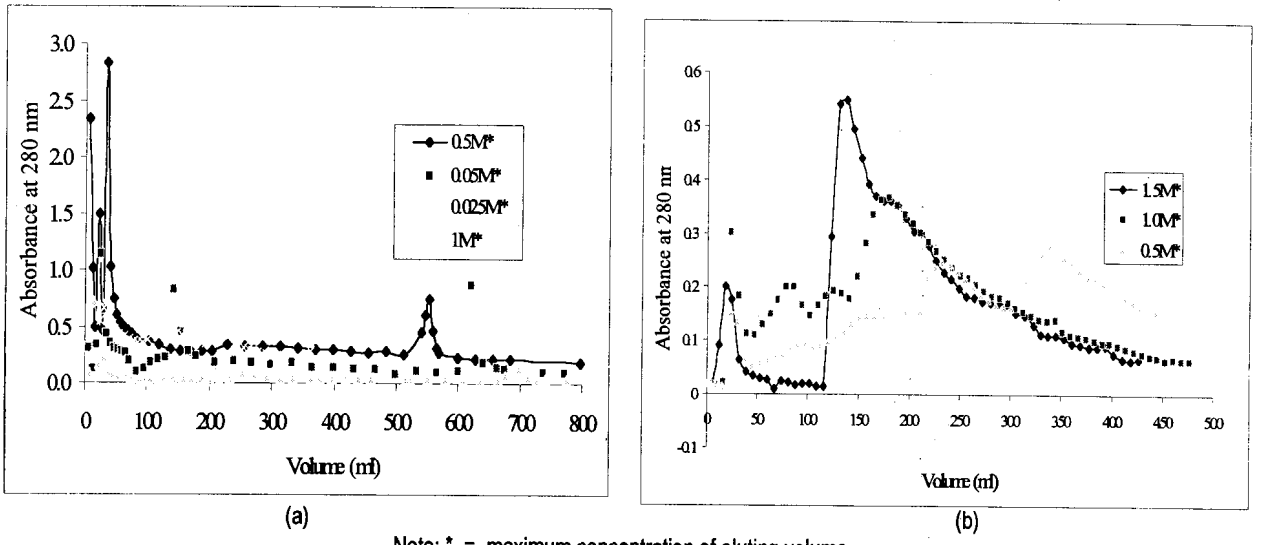

Note: * = maximum concentration of eluting volume

In the case of Amberlite IRA-410, the void volume, V_o (~20 ml) did not give the highest absorbance among the eluted fractions. However, there were still some colored products eluted at V_o. This is a different result from that using DOWEX 1-X8 where melanoidin was eluted at the void volume.

DEAE-Cellulose and DEAE-Sephadex are weakly basic anion exchangers and both showed the greatest capacity to decolorize melanoidin. There are advantages and disadvantages in using these two DEAE-resins. Both resins almost completely adsorbed the melanoidin. This was confirmed by not using salt gradient in the chromatographic run. Instead, phosphate buffer (pH 7, 0.005M) alone was used as eluent. A 19.89% and 0% melanoidin recovery were obtained for DEAE-Sephadex and DEAE-Cellulose, respectively.

Total salt concentrations of 1M and 0.5M for DEAE-Sephadex and 1.0M and 1.5M total salt concentration for DEAE-Cellulose were found to be the most effective for eluting melanoidin from the column. Table 2 shows this comparison.

Table 2. Melanoidin recovery using DEAE-Sephadex and DEAE-Cellulose at different salt concentrations.

Total Salt Gradient Conc. (M)	% Recovery	
	DEAE-Sephadex	DEAE-Cellulose
0	19.89	0
0.25	88.02	
0.5	100	83.94
1.0	100	100
1.5		95.33

DEAE-Sephadex gave a good melanoidin separation using 0.5M as the minimum salt concentration. However, this resin showed propensity to shrink with changes in salt concentration. In water, the soft dextran beads (to which the diethylaminoethyl groups have been attached) swell enormously due to repulsive forces within the polymeric molecules of the beads. The repulsive forces weaken as the salt concentration rises resulting in bead collapse (Scopes, 1987).

On the other hand, DEAE-Cellulose showed desirable adsorption characteristics. Unlike DEAE-Sephadex, this resin does not shrink with changes in salt concentration. All the loaded melanoidin was adsorbed and eluted with efficient separation using a 1M (minimum) total salt gradient concentration. The only problem encountered was the low flow rate for elution. A low flow rate of 2 min/ml was observed and ~15 hours were required for the elution of 500ml total volume of the eluent.

On the other hand, DEAE-Cellulose showed desirable adsorption characteristics. Unlike DEAE-Sephadex, this resin does not shrink with changes in salt concentration. All the loaded melanoidin was adsorbed and eluted with efficient separation using a 1M (minimum) total salt gradient concentration. The only problem encountered was the low flow rate for elution. A low flow rate of 2 min/ml was observed and ~15 hours were required for the elution of 500ml total volume of the eluent.

Furthermore, the performance of chitosan, a natural anion exchanger, was also tested for melanoidin decolorization. Unfortunately, majority of the melanoidin sample (43.53%) was eluted at the void volume, V_o. Therefore this material is not a suitable adsorbent for melanoidin.

The effect of buffer pH on the melanoidin decolorization was determined using natural melanoidin (Absolute Chemicals Inc., Lian Batangas). In the work of Monterey (2002), using DEAE-Cellulose at 1M total salt gradient concentration 56.1, 67.7 and 79.70% recovery values were obtained at pH 6, 7 and 8, respectively. Based on the results, one can see that as the pH was increased, the elution volume decreased. The pKa of DEAE-Cellulose is about 9.0-9.5 (Scopes, 1987); as the pH approaches 9.0, the resin's charge became less positive. Therefore as the pH increased, the resin became less positive, thus reducing the electrostatic attraction between sample and adsorbent.

It can be concluded that a lower pH allows for a more effective melanoidin decolorization since more positive sites on the adsorbent are available for binding at the lower pH. For the negatively-charged melanoidin, however, a higher pH is recommended (as long as the pKa of the anion exchanger is not exceeded) in order to achieve good separation of this color pollutant, as well as for the regeneration of the resin.

Ozonolysis

Ozone is a powerful reagent for cleaving the carbon-carbon double bonds of alkenes. It was known that melanoidin has the alkene functional group in its structure. Ozonolysis is a degradation reaction resulting in carbon-carbon double bond cleavage. The fragments formed would have a carbonyl functionality as a net result of the reaction. It is therefore a good tool for melanoidin decolorization. Figure 4 shows the mechanism of how ozone reacts with alkenes.

Figure 4 . Schematic representation of ozonolysis (Carey and Sunberg, 2001)

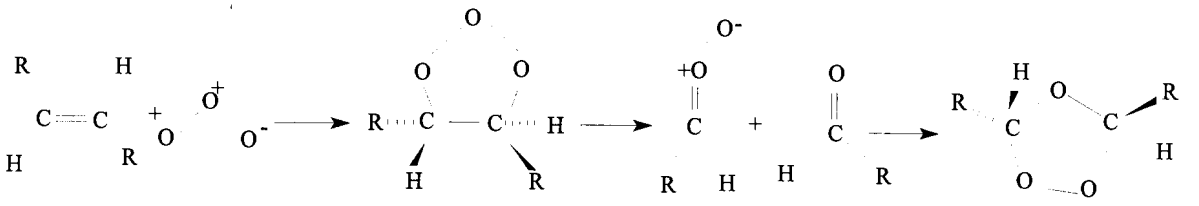

Macatangcay (2002) who studied the solvent free reactions between ozone and glycine-glucose melanoidin, achieved 29.26% and 32.14% absorbance reduction at 280 and 475 nm, respectively, and a MW reduction of 10.2% after 90 min of ozonation.

Solution viscosity can be used to measure the size or extension in space of polymer molecules. The simplicity of the measurement and usefulness of the viscosity-molecular weight correlation are so great that viscosity measurement constitutes an extremely valuable tool for the molecular characterization of polymers (Billmeyer, 1984). Viscometry was one of the methods used in order to determine the effectiveness of ozonolysis in degradation and decolorization of melanoidin.

The viscometer used in this study was of the Ubbelohde type and was calibrated using several standards (water, ethyl acetate and acetone) to determine the constants A and B for the equation

$$\eta = \left[A - \frac{B}{t^2} \right] \rho t$$

where η = viscosity (relative), t = time and ρ = density. This equation allows the determination of the effect of concentration on viscosity.

A purified sample of melanoidin was diluted into several concentrations (8.2×10^{-5}, 2.0×10^{-4}, 5.1×10^{-4}, 1.3×10^{-3}, 3.2×10^{-3} and 8.0×10^{-3} g/ml). It was shown in Figure 5 that the relative viscosity, η, decreased as the melanoidin concentration decreased.

Figure 5. Effect of concentration on the relative viscosity of melanoidin.

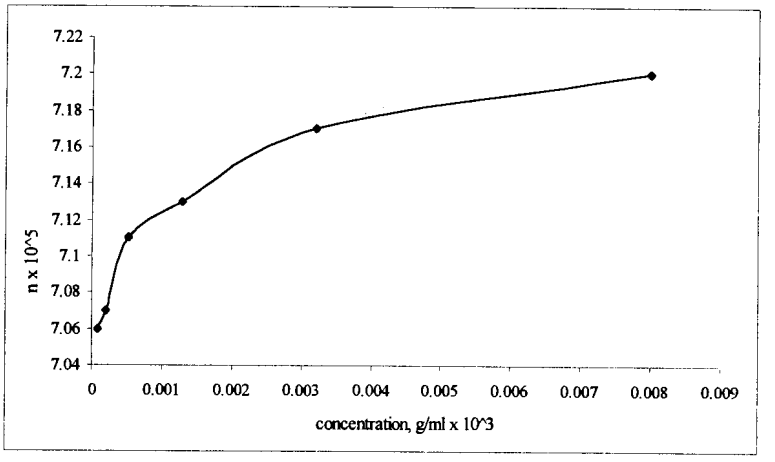

The average molecular weight $\overline{MW}$ of melanoidin can be determined using the Mark-Houwink equation.

$$[\eta] = K\overline{MW}^{a}$$

where $[\eta]$ = intrinsic viscosity

$\overline{MW}$ = average molecular weight

K, a = constants (dependent on the nature of the solvent and the temperature of the system)

This equation can be used to confirm if there was any degradation due to ozonolysis. Unfortunately, the viscometric properties of the ozonized melanoidin have not been determined.

Spectroscopic method was also used to determine the effect of ozonolysis on melanoidin decolorization. Based on the work of Macatangay (2002), a synthesized glucose-glycine melanoidin was ozonized for 45 mins. The absorbance at 280nm and 475nm of the ozonized and unozonized melanoidin were determined and compared. It was observed that there was a decrease in absorbance when the product was ozonized. He used Model 100 Sanders ozonizer (Kitigawa, Japan) for decolorization of solid melanoidin through ozonation. The elution profiles for ozonized and unozonized melanoidin can be seen in Figure 6. The unozonized melanoidin had a lower elution volume compared to the ozonized melanoidin, which means that the former has a higher $\overline{MW}$.

Figure 6. Elution profile of the ozonized and unozonized melanoidin using Sephadex G-75 column.

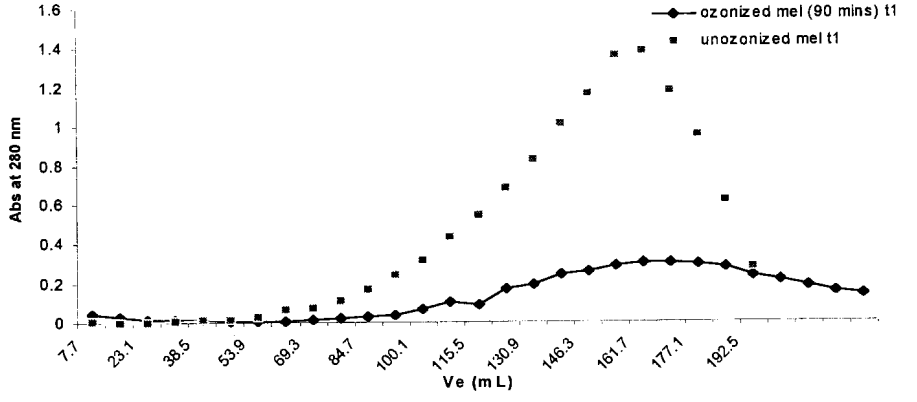

The results in Table 3 indicate that ozone was able to cleave the carbon-carbon double bond in melanoidin. Ozonolysis, therefore, is an effective method for melanoidin decolorization and can serve as a solution for the problem of dark-colored effluents.

Table 3. Effect of ozonolysis on decolorization of melanoidin.

	Weight melanoidin, g	Dilution, ml	Absorbance	
			280 nm	475 nm
Unozonized	0.24	100	0.915[a]	0.092[a]
	0.01	100	0.330	0.033
Ozonized	0.24	25	0.667[a]	0.064[a]
	0.01	25	0.107	0.022

a= further dilution: 1ml stock solution in 5ml

After ozonation, a 10.2 % reduction was observed in the $\overline{MW}$ of melanoidin (from 71732.46 Da to 64424.20 Da). This MW reduction can be attributed mainly to the depolymerization caused by ozone since it breaks the C=C bonds and converts them to carbonyl groups. The results generally support the Criegee mechanism (see Figure 7) as the mechanism for ozonation since the molecular weight distribution was significantly increased.

Figure 7. The Criegee mechanism (Bailey, 1978)

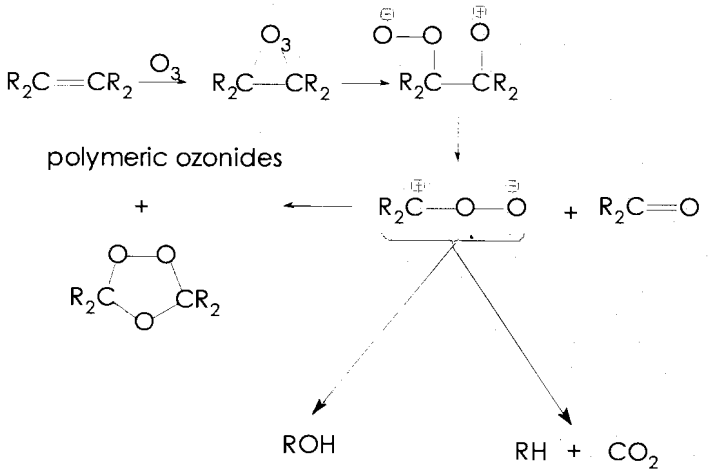

Using gel filtration chromatography, one can determine if there was melanoidin depolymerization due to ozonolysis. It is probable that the decolorization and the decrease in MW of melanoidin are due to cleavage of carbon-carbon bonds in their molecules by ozonolysis.

Natural melanoidin studied was obtained from alcohol distillery biodigester effluent. On the other hand, synthetic melanoidin was prepared by heating an equimolar mixture of glucose and glycine at 160°C for two minutes. The average molecular weights (MW) of the melanoidin samples were determined using a G-75 Sephadex column (MW Range = 10000-70000 Da). Since there are no known standards for the analysis of melanoidin (its structure has not yet been established), protein standards were used. In using protein standards, it is assumed that the melanoidin has a molecular size or weight within the range of the protein standards. From the results, the molecular weight was found to be 77kDa for natural and 61 kDa for synthetic melanoidin.

Salt gradient elution (with final NaCl concentration of 1.5M) resulted in 95.3% total recovery of synthetic melanoidin after adsorption by DEAE-cellulose. The computed values of the decolorization of the distillery effluent, in which the decolorization was equal to melanoidin adsorption and recovery by gradient elution, and the melanoidin elution at the specified NaCl concentration was optimal, were 56.1 $\pm$ 0.8% (0.64M NaCl) at pH 6, 67.7% $\pm$ 1.0% (0.31 M NaCl) at pH 7 and 79.7% $\pm$ 1.4% (0.29M NaCl) at pH 8. Thus, melanoidin adsorption by DEAE-cellulose at pH 8 was most effective in decolorizing alcohol distillery effluent.

The Huggins' plot was constructed and is presented in Figure 8 (next page). It can be seen on the plot that the intercept (which corresponds to the intrinsic viscosity of the melanoidin-water system) was negative, a result that has no physical significance and is therefore not allowed. This dilemma has no definite explanation at the moment (Rosenthal, 1994) and could be partly due to the extreme poly dispersity of the melanoidin solution. However, the magnitude of the intercept has a correlation with the MW's for the two systems (the melanoidin-water and the ozonized-melanoidin-water systems); based on the observed correlation coefficients, there was a significant decrease in the intercept values for the two systems. At the same concentrations for the two systems, the intrinsic viscosity generally decreases upon ozonation since the unozonized melanoidin exhibited higher η_{sp}/c values than the ozonized melanoidin.

Figure 8. Determination of Intrinsic Viscosities of the Unozonized and Ozonized glucose-glycine melanoidin

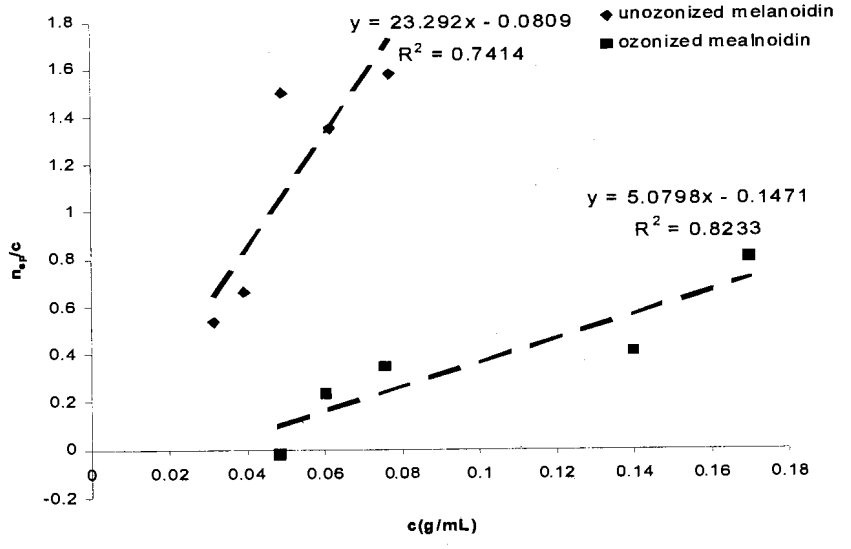

Evaluation of the agreement of the column chromatography with the viscometry measurement results was also done. Approximations were made to establish a mathematical explanation of the observed MW reduction (~10.2 %) in gel column chromatography in terms of viscosity. It was found that the ratio of the *a* values for the unozonized and ozonized (a_{unozo}/a_{ozo}) was equal to 1.07. This indicates good correlation between geometry and MW for both the unozonized and ozonized melanoidin. Also, it indicates slight change in the geometry of the melanoidin molecules after ozonation.

As seen in Table 5, the strength of the C=C stretch was reduced significantly after ozonation. The ozonation did not convert all C=C bonds into carbonyl or carboxylic groups since the C=C stretch did not disappear, which agrees with the efficiency of ozonation/decolorization obtained from the UV-VIS data. The presence of the carbonyl/carboxylic peak in the spectra supports the Criegee mechanism for ozonation.

Table 5. Comparison of the major functional groups for unozonized and ozonized melanoidins based on IR spectral results

Functionality	Unozonized melanoidin (absorption wave number, intensity)	Ozonized melanoidin (absorption wave number, intensity)
C=C stretch	1647.81, medium	1633.47, weak
O-H stretch	3404.78, strong	3440.64, medium
C-O stretch	1081.27, strong; 1389.64, weak	1081.27, weak; 1375.30, strong
C=O stretch	N/A	1726.69, weak

Kinetic models for reaction of ozone and melanoidin

➢ Determination of the reaction order

A plot of absorbance at 475 nm against time during decolorization of melanoidin was prepared. The rate was calculated from the slope of the tangent to the curve.

The reaction rate was measured at the beginning of the reaction for several different initial concentrations of reactants. The rate law for a reaction is given by the equation:

$$v = kM^n \quad (1)$$

Taking natural logarithms:

$$\ln v = \ln k + n \ln M \quad (2)$$

where M = initial concentration of melanoidin
v = initial velocity
n = reaction order

A plot of the natural logarithm of the initial rate, ln v, against the natural logarithm of the initial concentration, ln M should be a straight line with slope equal to the reaction order n.

➢ Determination of rate constant

The concentration of ozone was in excess and was assumed to be constant throughout the reaction.

$$M + O_3 \rightarrow \text{Product} \quad (3)$$

$$\frac{-dM}{dt} = kO_3 M^n = k'M^n \quad (4)$$

Equation (4) may be rearranged to give:

$$\frac{dM}{M} = -kdt \quad (5)$$

which can be integrated directly because k is independent of t. Initially (at t = 0) the concentration of M was Mo; at a later time t it was M, using these integration limits:

$$\int_{M_o}^{M} dM = -\int_0^t k'\,dt \quad (6)$$

$$\frac{1}{(1-n)}\left[M^{(1-n)} - Mo^{(1-n)}\right] = -k't \quad (7)$$

$$M^{(1-n)} - Mo^{(1-n)} = -(1-n)k't \quad (8)$$

$$M^{(1-n)} = Mo^{(1-n)} - (1-n)k't \quad (9)$$

A plot of $M^{(1-n)}$ against t should be a straight line with slope - (1-n) k'. From the slope, the rate constant may be calculated once the order of the reaction (n) has been determined.

➢ Reaction Order

The time course of the absorbance at 475 nm during decolorization of melanoidin by ozonolysis at different pH was observed. The decolorization of melanoidin increased markedly at the initial stage of ozonolysis and remained constant thereafter.

Initial rates were determined for different initial concentrations of melanoidin. A plot of the logarithm of the initial slope against the logarithm of melanoidin concentration gave a slope which corresponds to the order of the reaction. Table 8 shows the reaction order at different pH values. It can be seen that the reaction of ozone with melanoidin has a kinetic order of one; therefore, the reaction is pseudo-first order with respect to melanoidin. The kinetic order with respect to ozone was not determined.

Table 8. Reaction order for ozone reaction with melanoidin at different pH.

pH	Reaction order		
	Trial 1	Trial 2	Average
3.5	0.92	0.92	0.92 ± 0.00
5.0	0.88	1.14	1.01 ± 0.13
6.5	1.16	0.78	0.97 ± 0.19
7.0	1.36	1.15	1.26 ± 0.10
8.5	1.39	1.10	1.25 ± 0.15
10.0	1.52	1.22	1.37 ± 0.15

➢ Rate Constant

Values of the pseudo-first order rate constant k' were determined using equation 8. Table 9 shows the rate constant at low and high pH values and ranged from 0.16 to 0.37 min^{-1}; unfortunately, there was no distinct trend in the values of the rate constant with pH.

Table 9. Rate constants of ozonolysis of melanoidin at different pH

pH	Rate constant (min^{-1})
3.5	0.21 ± 0.03
5.0	0.28 ± 0.04
6.5	0.24 ± 0.11
7.0	0.37 ± 0.09
8.5	0.16 ± 0.02
10.0	0.35 ± 0.07

Microbial Decolorization

It was observed that after the bacterial treatment, there was a significant decrease in the absorbance of each sample. The actual MDA values are presented in Table 6. The OZO-15 sample yielded the highest extent of decolorization, followed by OZO-30 which gave 35.65% decolorization after five days of inoculation. The decolorization value for OZO-60 ranged from 22-24% from day 1 to day 5 after inoculation. The extent of decolorization was monitored every 24 hours. It was noted that the fluctuation of absorbance was 0.424-0.440 at 475 nm. *Bacillus subtilis* was expected to effectively decolorize the samples (which were exposed to ozonation for a shorter duration) since the melanoidin structure was not yet substantially cleaved.

Table 6. The computed percent melanoidin decolorizing activity (MDA) of microbially treated melanoidin.

	%MDA									
Sample	day1		day2		day3		day4		day5	
	trial 1	trial 2	trial 1	trial 2	trial 1	trial 2	trial 1	trial 2	trial 1	trial 2
BAC-OZO-stock	34.91	35.48	42.38	39.21	46.52	41.27	57.00	43.00	61.81	51.06
BAC-OZO-15	32.29	32.03	39.92	29.55	42.59	35.04	43.21	37.96	45.25	46.28
BAC-OZO-30	16.75	19.22	22.53	25.13	26.97	30.18	29.63	32.97	32.51	38.77
BAC-OZO-60	23.87	23.50	23.69	23.33	22.26	22.98	24.59	23.33	22.80	22.80

The pH of the sample is expected to affect the decolorizing activity of *Bacillus sp.* since its growth depends on the sample pH. Also, the enzymes produced by the bacteria, which are responsible for melanoidin decolorization, is pH dependent. OZO-60 gave the lowest pH value (4.58) after 60 minutes of ozonation, which may have lead to bacterial cell death and lack of enzyme activity. This may be the primary reason why the MDA did not increase anymore and just fluctuated within the range mentioned above. The scope of the study, however, did not include measuring and identifying the specific activity and identity of the enzyme produced by the bacterium.

The MW of the dialyzed melanoidin was found to be 51.57 kDa. MW values of ozonated and microbially treated melanoidin after ozonation is shown in Table 7.

Table 7. MW values of ozonated and microbially treated melanoidin after ozonation

Sample	MW, kDa		Sample	MW, kDa	
	trial 1	Trial 2		trial 1	trial 2
OZO-stock	23.35	22.22	BAC-OZO-stock	19.75	18.93
OZO-15	18.79	17.67	BAC-OZO-15	16.58	15.90
OZO-30	15.27	15.00	BAC-OZO-30	13.23	13.48
OZO-60	8.95	8.37	BAC-OZO-60	7.84	7.38

The elution profiles of bacterially-treated and untreated ozonated melanoidin at different time intervals are shown in Figures 9-11. Bacterial treatment was done with *Bacillus sp.*

Figure 9. Elution profile of ozonated melanoidin at different time interval (15, 30 qnd 60 mins).

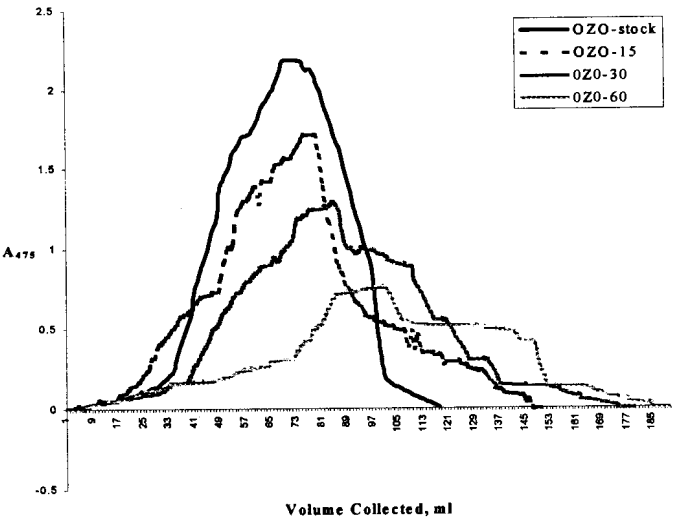

Figure 10. Elution profile of ozonated melanoidin treated with *Bacillus sp.*

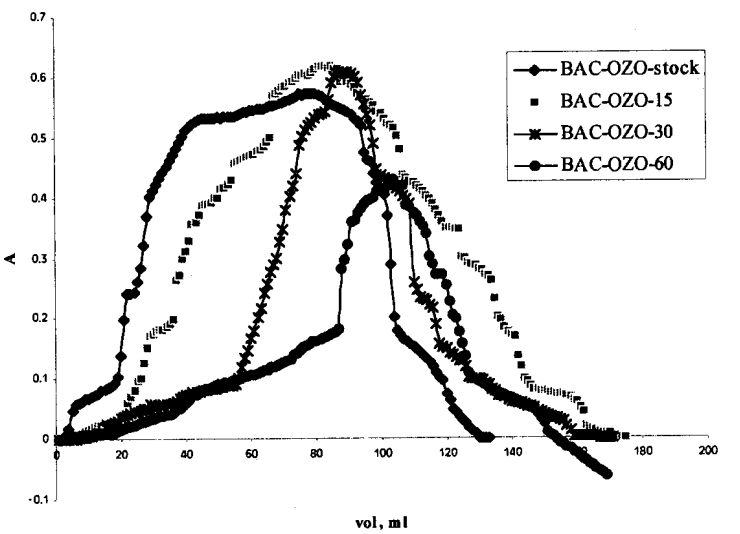

Figure 11. Elution profile of dialyzed melanoidin.

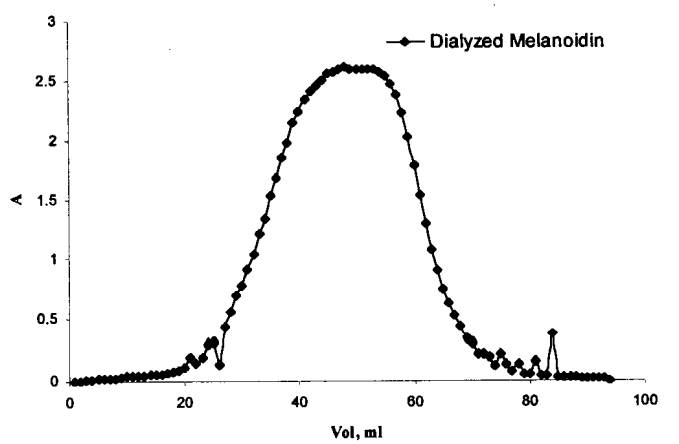

The UV-Vis spectra of the various ozonated melanoidin (OZO-stock, OZO-15, OZO-30, and OZO-60) are shown in Figure 12. The spectra showed a significant change in absorption intensity of the ozonated melanoidin relative to those of the unozonated melanoidin, Peaks were observed at 200-700 nm. This is in agreement with the experimental results of Belina (2004).

Figure 12. UV-VIS spectra of bacterially treated melanoidins that were exposed to ozone at different time interval (15, 30 and 60 mins).

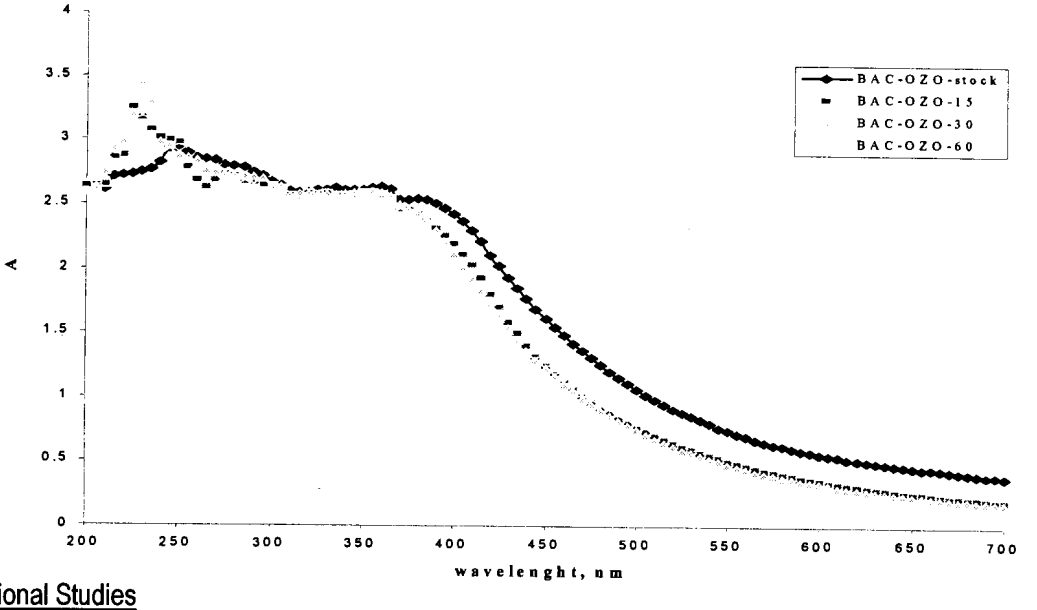

Computational Studies

Computational chemistry was used to determine the most probable pathway for the ozonation of melanoidin. Using the software HyperChem®, the thermodynamic stability, as well as orbital calculations, of the reaction intermediates and products was determined. The calculations basically examine potential energy surfaces with single point calculations, optimization and molecular dynamic simulation.

HyperChem® uses two computational methods: molecular mechanics and quantum mechanics. There are two Quantum Mechanical (QM) methods used in computational chemistry. The first one is the *ab initio* calculation which solves the Schrödinger equation without using empirical data and the second is the semi-empirical method wherein assumptions are incorporated in order to fit some established experimental results.

Changes in the heat of formation during the initial stage of the Maillard reaction until the formation of the rearrangement compound were also considered. This is very crucial since the rearrangement compound (Amadori/ Heyns) is a common intermediate for the formation of the three proposed melanoidin product. Table 10 shows the calculated heat of formation using the semi-empirical PM3 method. Values of the equilibrium constant (K_{eq}) were calculated (Table 11) for the following reaction scheme:

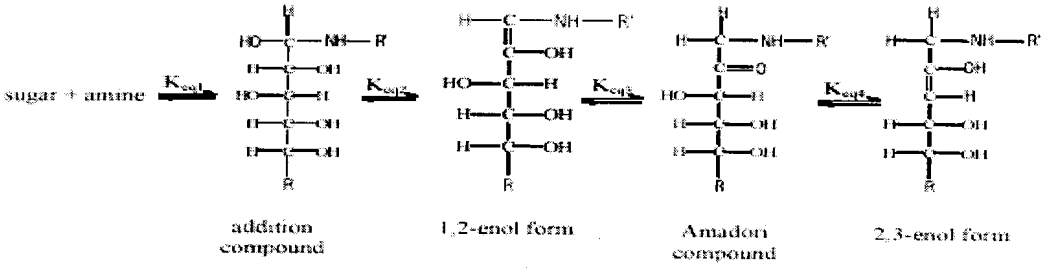

where K_{eq1}, K_{eq2}, K_{eq3} and K_{eq4} correspond to the equilibrium reaction step in the given scheme.

Table 10. ΔH_f° of intermediate products during the formation of the Amadori/ Heyns rearrangement product.

Model System	Heat of Formation (kcal/ mol)					
	At infinite separation	Add'n compound	Schiff base	1,2-enol form	Rearrangement Product	2,3-enol form
Xylose-glycine	-310.6	-314.0	-256.7	-256.9	-265.3	-260.8
glucose-glycine	-361.5	-363.5	-302.5	-302.8	-308.6	-302.3
fructose-glycine	-358.8	-364.4	-301.9	-302.2	-304.8	-301.2

Table 11. Equilibrium constants for the formation of the rearrangement products

Model System	K_{eq} values			
	K_{eq1}	K_{eq2}	K_{eq3}	K_{eq4}
Xylose-glycine	309.0	1.5×10^{-42}	1×10^{6}	5×10^{-4}
Glucose-glycine	29.2	3.5×10^{-45}	1.8×10^{5}	2.4×10^{-5}
Fructose-glycine	1.3×10^{3}	2.8×10^{-46}	112.3	1.6×10^{-3}

The Gibbs energy change equation for the reaction in an isentropic system was used in computing the equilibrium constants. Based on the computed heat of formation and equilibrium constants, formation of the addition and the rearrangement compounds were observed to be favored.

Using the semi-empirical PM3 method, the melanoidin structures were optimized and the heat of formation and orbital energies were computed (Tables 13 and 14, respectively). The heats of formation of melanoidin, expressed in kcal/ gram, were compared. Using the kcal/ gram as basis for comparison takes into account the possible inconsistencies in defining the monomeric component of the polymeric product. Also, during polymerization, it was found that the heat of formation on a per mole basis generally increases.

The three equivalent melanoidin structures (KT, CK and YK), which were used in the calculations, consist of four sugar units and four amine units as the repeating component. Comparisons using the equivalent structures ensure that the entropy terms are comparable among the proposed melanoidin products for all model systems. Hence, a tetramer of YK product and a monomeric unit each of KT and CK polymers were considered during the comparative computations.

Ozone is commonly used in decolorizing wastewater due to its strong oxidizing capability and cleaves alkenes to aldehydes and/or ketones. It is very unstable as shown by its high heat of formation (51.056 kcal/ mol or 1.064 kcal/ g). The basic mechanism of ozonolysis was formulated by Criegee (McMurry, 2000). Electrophilic attack by ozone proceeds through a six-electron transition state forming the primary ozonide or molozonide, a compound containing two weak oxygen-oxygen bond. This compound is relatively unstable and rearranges to an ozonide.

Table 13. Calculated ΔH_f of ozonolysis intermediates and products (*in vacuo*) based on Y-K, K-T and C-K structures of two model systems.

Fructose-Glycine Model System

Compounds	*Heat of Formation (kcal/ g)*		
	Y-K	*C-K*	*K-T*
Melanoidin	-1.17	-0.95	-1.11
Ozone + Melanoidin	-1.03	-0.84	-1.00
Ozone (2 moles) + Melanoidin	-0.90	-0.74	-0.89
Molozonide	-1.09	-0.82	-1.05
Molozonide (2 sites of reaction)	-1.02	-0.85	-0.96
Ozonide	-1.19	-0.97	-1.10
Ozonide (2 sites of reaction)	-1.21	-1.00	-1.10
Intermediate Reaction Products:			
Product A	-1.27	-0.96	-1.23
Product B	-1.25	-1.05	-1.09
Product C	-1.20	-0.98	-1.11
Product D	-1.35	-1.11	-1.18
Product E	-1.39	-1.29	-1.25

Glucose-Glycine Model System

Compounds	*Heat of Formation (kcal/ g)*		
	Y-K	*C-K*	*K-T*
Melanoidin	-1.19	-0.97	-1.09
Ozone + Melanoidin	-1.04	-0.86	-0.96
Ozone (2 moles) + Melanoidin	-0.91	-0.75	-0.85
Molozonide	-1.11	-0.90	-1.02
Molozonide (2 sites of reaction)	-1.03	-0.86	-0.97
Ozonide	-1.20	-0.99	-1.11
Ozonide (2 sites of reaction)	-1.22	-1.00	-1.13
Intermediate Reaction Products:			
Product A	-1.15	-1.03	-1.17
Product B	-1.28	-1.11	-1.15
Product C	-1.17	-1.28	-1.12
Product D	-1.35	-0.99	-1.30
Product E	-1.38	-1.10	-1.23

Table 14. Calculated orbital energies and HOMO-LUMO gap for melanoidin ozonolysis of two model systems.

Fructose-Glycine Model System

Orbital Energies, eV

	Y-K		*K-T*		*C-K*	
	HOMO	*LUMO*	*HOMO*	*LUMO*	*HOMO*	*LUMO*
Ozone	-12.03	-2.23	-12.03	-2.23	-12.03	-2.23
Melanoidin	-8.73	-0.45	-8.28	-0.49	-9.46	-0.59

HOMO-LUMO gap, eV

Melanoidin as nucleophile	6.50	6.05	7.23
Ozone as nucleophile	11.58	11.54	11.44

Glucose-Glycine Model System

Orbital Energies, eV

	Y-K		*K-T*		*C-K*	
	HOMO	*LUMO*	*HOMO*	*LUMO*	*HOMO*	*LUMO*
Ozone	-12.03	-2.23	-12.03	-2.23	-12.03	-2.23
Melanoidin	-9.24	-0.31	-8.26	-0.27	-9.53	-0.04

HOMO-LUMO gap, eV

Melanoidin as nucleophile	7.01	6.03	7.3
Ozone as nucleophile	11.72	11.76	11.99

To determine the most probable and stable structure that reacts with melanoidin during ozonation, different structures of ozone were subjected to geometry optimization and calculations. Among the three algorithms used (*ab initio*, DFT and PM3), PM3 (parametric method 3) produced the most negative total energy, which is considered the most thermodynamically stable, as shown in Table 12. The energy values calculated among the five structures were almost the same.

Table 12. Comparison of the total energy of ozone using different methods of calculation

	Structure	Total Energy (kcal/mol)		
		PM3	*ab initio*	DFT
Structure 1	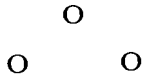	-20145.17	-138861.35	-139519.26
Structure 2	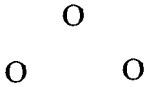	-20145.17	-138861.19	-139519.29
Structure 3	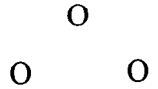	-20061.99	-138452.85	-139034.52
Structure 4	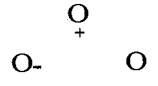	-20145.17	-138861.19	-139519.29
Structure 5		-20145.17	-138861.19	-139519.29

The three proposed structures of melanoidin and the intermediate and reaction products of ozonolysis are shown in Figures 13 to 15.

Figure 13. Yaylayan-Kaminsky (Y-K) structures of melanoidin and intermediate products after ozonolysis

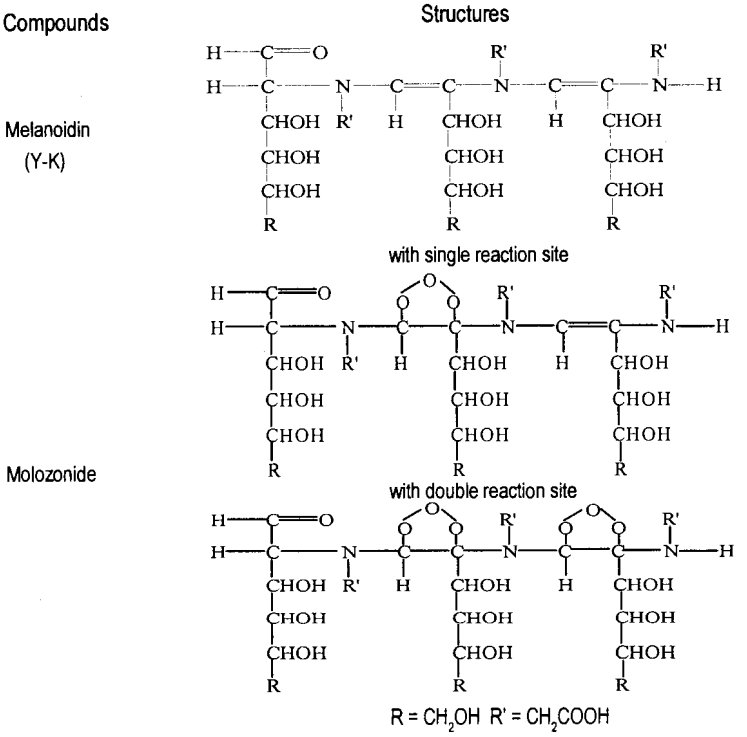

with single reaction site

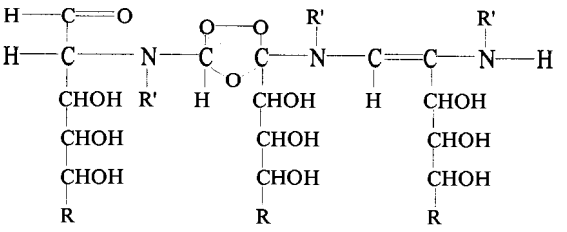

Ozonide

with double reaction site

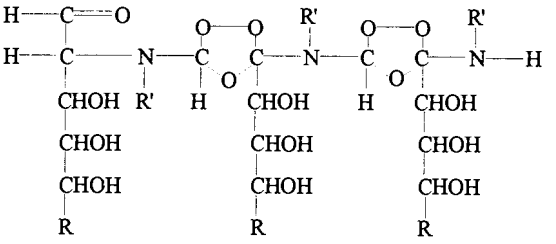

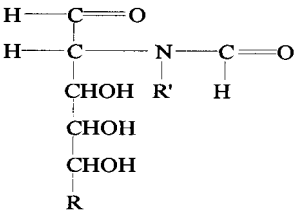

product A

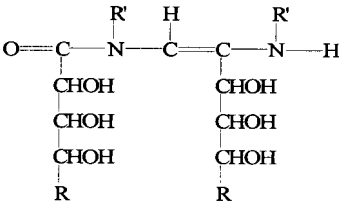

product B

Intermediate Reaction Products

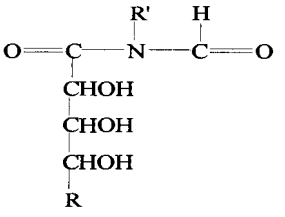

product C

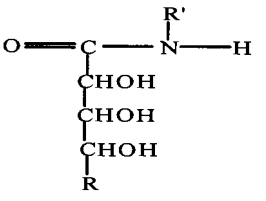

product D

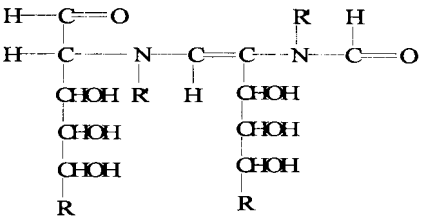

product E

Figure 14. Kato-Tsuchida (K-T) structures of melanoidin and intermediate products after ozonolysis

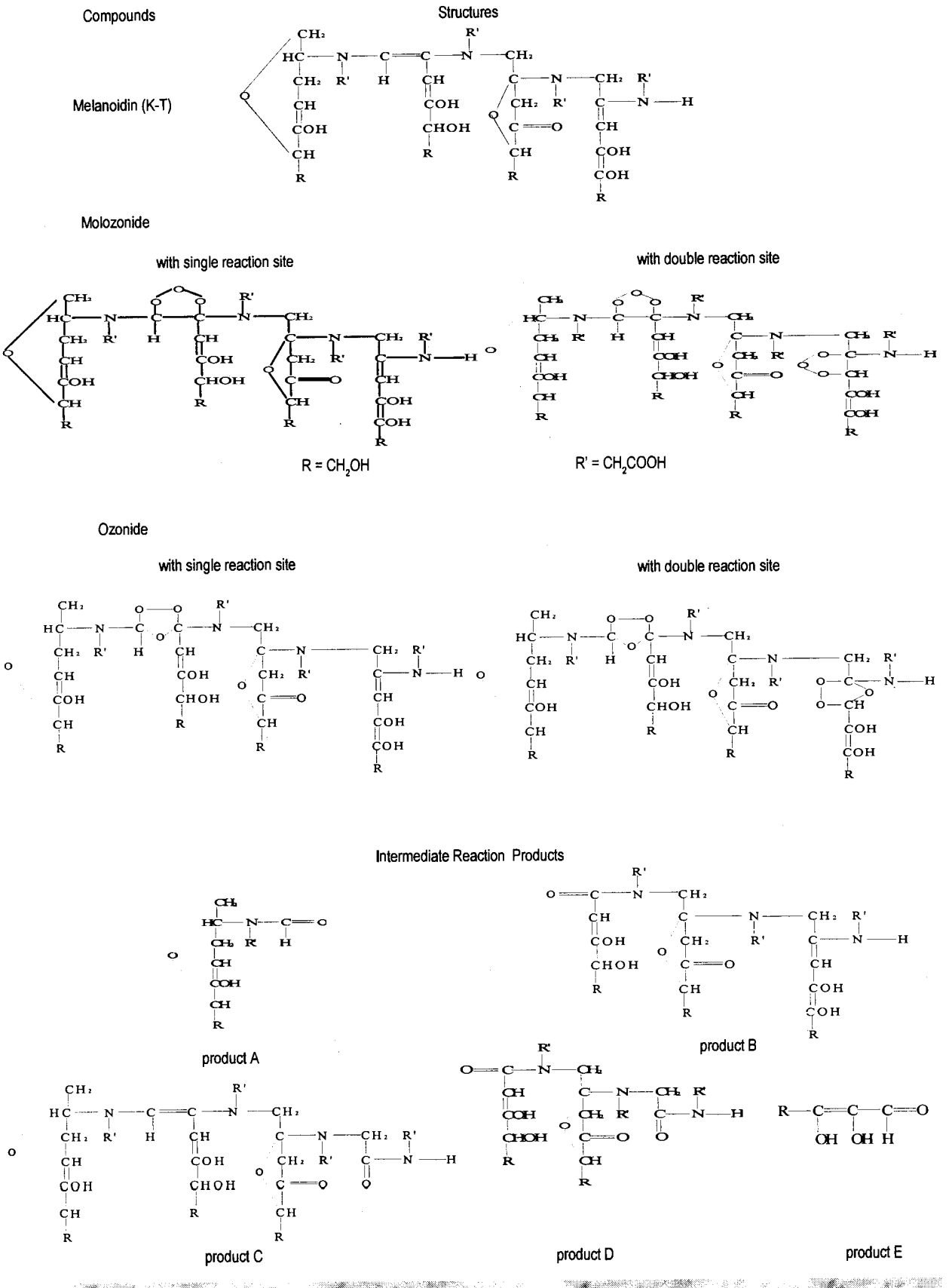

Figure 15. Cammerer-Kroh (C-K) structures of melanoidin and intermediate products after ozonolysis

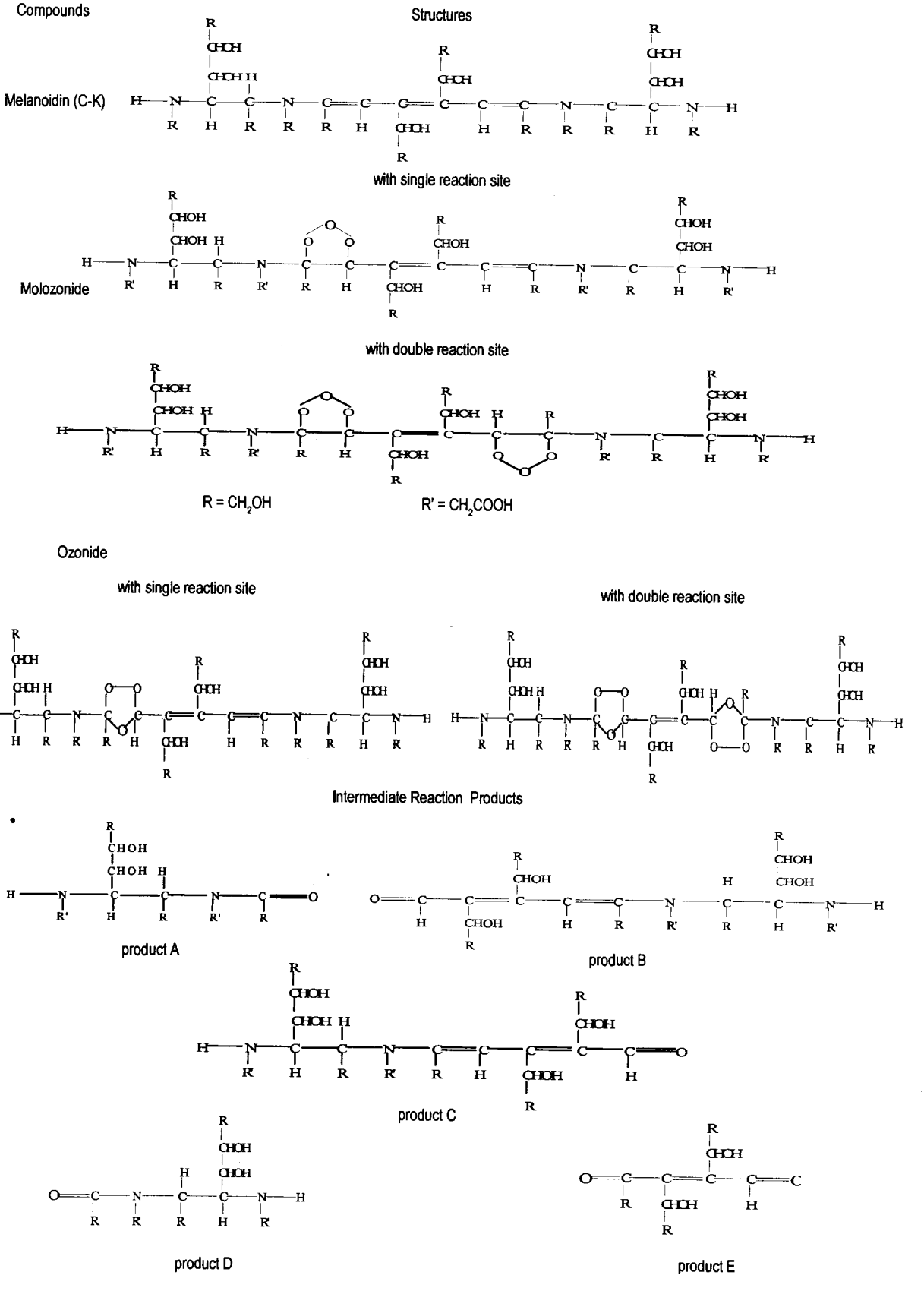

Tables 13 shows the heat of formation of the ozonation intermediates and products (*in vacuo*) of the three proposed structures of melanoidin. The Y-K structures have the least (more negative) values of ΔH°_{f}. This indicates that the ozonation mechanism based on the Y-K structure lead to products that are thermodynamically more stable compared to that based on the C-K and K-T structures.

Frontier Molecular Orbitals (FMO) are the orbitals that predominantly participate in chemical reactions. FMO consist of the Highest Occupied Molecular Orbital (HOMO) and the Lowest Unoccupied Molecular Orbital (LUMO). Evaluating reactivity on the basis of FMO predicts the possible product formation but does not confirm a non-occurrence of a particular reaction. In Table 14, the HOMO-LUMO gap and orbital energies of reaction products and intermediates in glucose-glycine and fructose-glycine model systems are presented.

Reactions are likely to occur if the molecular orbitals have strong interactions, which means that the energies of the orbitals must be closer. The values of the HOMO-LUMO energy gap of melanoidin for the fructose-glycine model system were smaller compared to those of the glucose-glycine model system. Thus, the formation in the fructose-glycine model system was favored over the other model system. Melanoidin acting as nucleophile gave low HOMO-LUMO energy gap indicating that this would be the probable mechanism.

The Frontier Molecular orbital plots and coefficients of the three proposed melanoidin structures are Figure 16 – 18. Electrons tend to be more localized around atoms with high molecular orbital coefficients, thus, indicates where new bonds are likely to form. High molecular coefficients (regardless of their signs) were obtained for the C=C bond and the nitrogen atom. Furthermore, the HOMO and LUMO plots show that the electrons are concentrated in the ethylenic compound (C=C) for the LUMO and in the nitrogen atom for the HOMO (as shown by large orbital lobes). These plots determine the possible reactive sites in melanoidin

Figure 16. Frontier Molecular Orbital plots and coefficients for Y-K melanoidin structure (fructose-glycine-glucose model system)

Atomic Cores

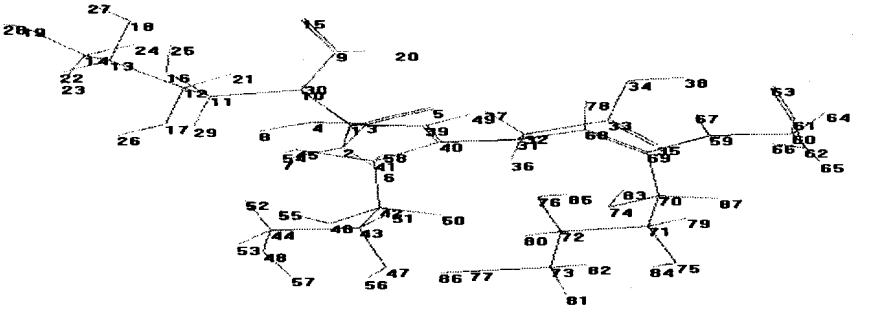

LUMO (-0.45 eV)

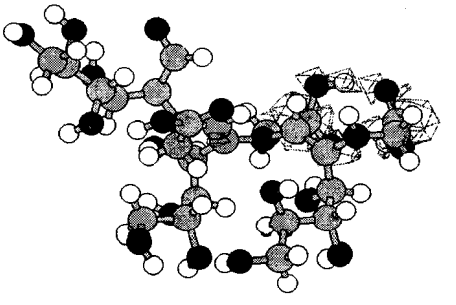

HOMO (-8.73 eV)

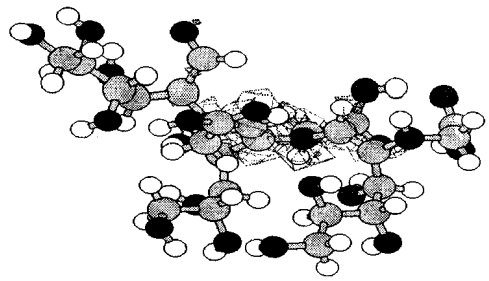

	N31S	C32S	C32Pz	C33S	C33Py	C33Pz	O34Px
	0.17	-0.13	-.012	0.16	-0.30	-0.50	0.13
LUMO	O34Pz	O35Py	O35Pz	C39Py	C40Px	C61S	C61Px
	0.13	0.22	0.31	0.12	0.14	0.12	-0.27
	C61Py	C61Pz	O62Py	O63Px	H66S	H38S	
	-0.12	0.20	0.12	0.19	0.11	0.15	

	N1Py	N1Pz	N31Px	N31Py	N31Pz	C39Px	C39py
	0.17	-0.30	-0.32	0.52	-0.18	0.11	-0.44
HOMO	C40Py	N59Py	C68Py	C69Px	H36S	H37S	H78S
	-0.21	0.11	-0.11	-0.14	-0.11	0.12	0.12

Figure 17. Frontier Molecular Orbital plots and coefficients for K-T melanoidin structure (fructose-glycine model system)

Atomic Cores

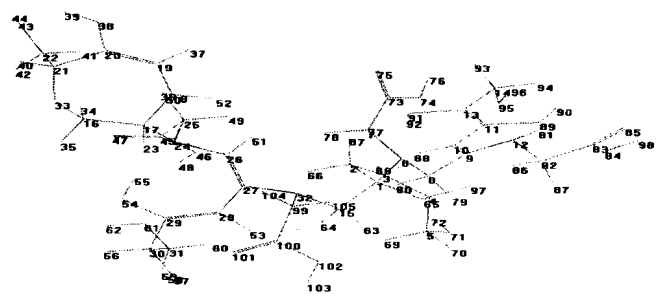

LUMO (-0.49 eV)

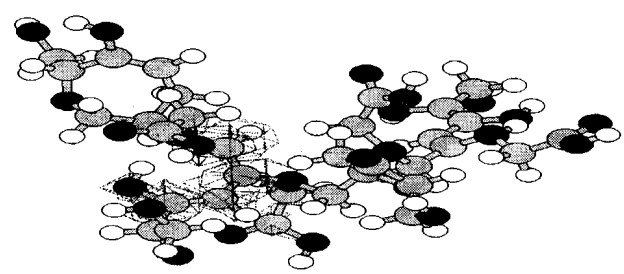

HOMO (-8.28eV)

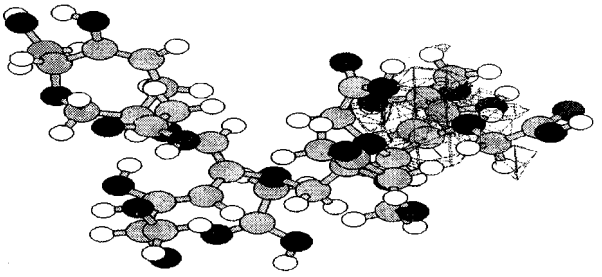

Orbital Coefficients

LUMO	C26Px	C26Py	C26Pz	C27Px	C27Py
	-0.17	-0.46	0.28	0.13	0.42
	C27Pz	C28Py	C29Py	O54Py	
	-0.26	0.24	-0.49	.018	

HOMO	C9Px	C9Py	C9Pz	C10Px	C10Py	C10Pz
	0.16	-0.26	-0.12	0.21	-0.33	-0.20
	C11Py	N12S	N12Px	N12Py	N12Pz	C13Px
	0.28	0.18	-0.13	.041	0.18	-0.15
	C13Py	O89Py	O91Px	O91Py	H87S	
	0.44	-0.13	0.14	-0.14	0.11	

Figure 18. Frontier Molecular Orbital plots and coefficients for C-K melanoidin structure (fructose-glycine model system)

Atomic Cores

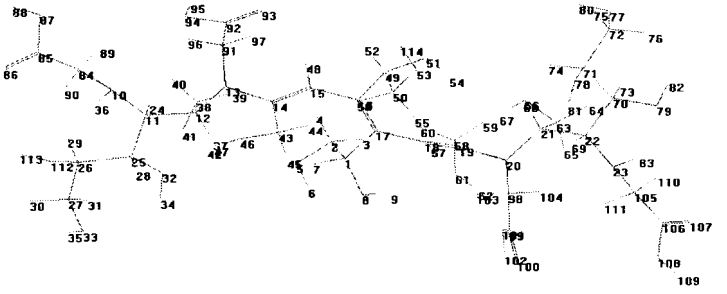

LUMO (-0.59 eV)

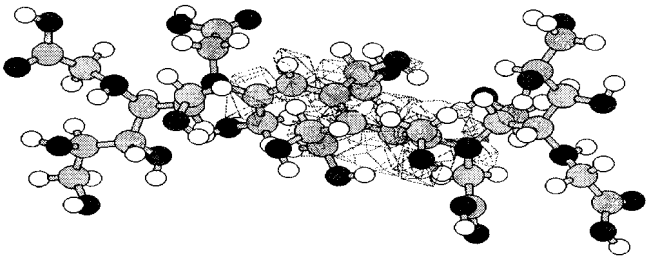

HOMO (-9.46 eV)

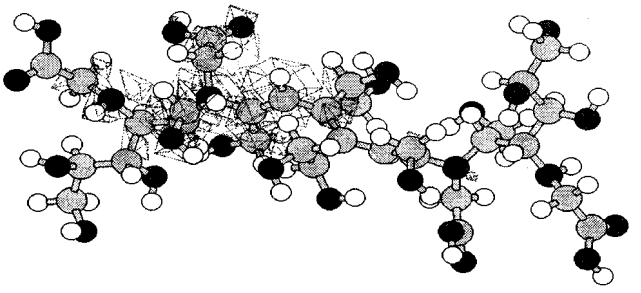

Orbital Coefficients

LUMO	C14Pz	C15Pz	C16Px	C16Py	C16Pz	C17Px	C17Py
	0.15	-0.13	0.17	-0.31	-0.25	-0.20	0.27
	C17Pz	C18Px	C18Py	C18Pz	C19Px	C19Py	C19Pz
	0.16	-0.31	0.29	-0.24	0.35	-0.27	0.29

HOMO	N10Py	C12Pz	N13S	N13Py	N13Pz	C14Px	C14Pz
	-.020	-0.16	-0.23	0.47	0.47	-0.12	-0.23
	C15Px	C15Py	C15Pz	C38Pz	H97S		
	-0.13	0.13	-0.36	0.10	-0.14		

Most of the time, chemical reactions take place in the liquid or solid phase. But isolated gas phase molecules are the simplest to treat computationally. To treat these condensed phases, one must simulate continuous, constant density, macroscopic conditions. HyperChem uses the TIP3P water model for solvation. The solute is placed in a box of TIP3P water molecules with imposed periodic boundary conditions. The water molecules used to solvate a solute comes from Jorgensen's Monte Carlo equilibrated box model (1983).

Solvation has profound effects on the results of a chemical calculation. The molecules have polar groups that exhibit solvent-solute interactions. Hydrogen bonding can actively participate in the reaction. The solvent strongly influences the energies of different solute conformations. The nature of solute-solute and solute-solvent interactions is dependent on the solvent environment. Solvent influences the hydrogen-bonding pattern, solute surface area and hydrophilic and hydrophobic group exposures. There is an intense effect of solvation on the calculated ΔH°_{f} making these values more negative, i.e. making the system more energetically stable.

The number of water molecules added to the solute depends on its size and its orientation. The effect of increasing number of water molecules on the heat of formation was done (see Table 15 and Figure 19).

Table 15. Heat of Formation of Solvated Neutral Glycine (computed using different Force Fields)

Number of Water Molecules	*(actual number of H_2O molecules)* Heat of Formation (kcal/ mol)			
	OPLS	BIO+CHARMM	MM+	AMBER
0	-89.842	-86.759	-89.810	-91.747
~ 50	*(50)* –2825.522	*(49)* –2730.464	*(50)* -2664.022	*(50)* -2786.740
~ 100	*(105)* -5258.579	*(105)* -5149.966	*(105)* -4938.846	*(105)* -5173.845
~ 150	*(150)* -8354.144	*(149)* -8283.401	*(150)* -7845.972	*(149)* -8220.789
~ 200	*(210)* –11622.742	*(210)* -11631.542	*(210)* -11094.163	*(210)* -11519.815
~ 250	*(259)* –14347.128	*(258)* -14349.514	*(259)* -14377.491	*(258)* -14239.448
~ 300	*(308)* –17170.827	*(308)* -17223.963	*(308)* -16304.686	*(308)* -17041.330
~ 350	*(358)* –20046.841	*(361)* -20008.109	*(362)* -20034.968	*(361)* -19881.670
~ 400	*(404)* –22359.856	*(404)* -22481.586	*(404)* -21450.079	---

Figure 19. Effect of increasing water molecules on the Heat of Formation of solvated neutral glycine

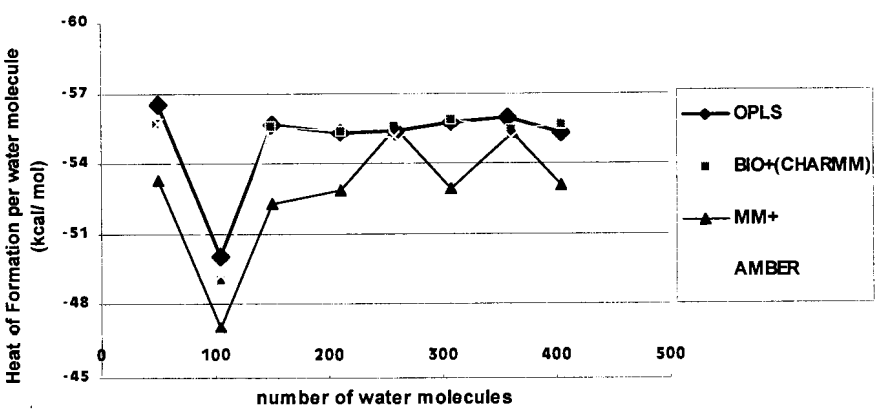

As shown in Table 15, the presence of solvent molecules made a drastic increase in the heat of formation of the solute. Thermodynamically, this indicates that the solvated system is more stable than the system *in vacuo*.

No specific trend or behavior was exhibited by the calculated heats of formation of neutral glycine solvated with less than 200 water molecules. Above 200 water molecules, the heat of formation seemed to follow a linear relationship; thus, these points (from ~200 to ~350 water molecules) were subjected to linear regression. Table 16 shows the computed slope and correlation coefficients of these points.

Among the force fields, OPLS has the highest correlation coefficient, indicating that the heat of formation of neutral glycine computed using OPLS has a linear relationship with the number of water molecules. The small values of slope indicated the minimal change in the heat of formation. Thus, the properties of solvated system containing 200 to 350 water molecules may be computed using the OPLS force field.

Three model systems (fructose-glycine, glucose-glycine and xylose-glycine) for three proposed structures of melanoidin, which have been proposed in the literature, were solvated with 200 to 220 water molecules and their heats of formation were computed using HyperChem. The structures were first optimized using the OPLS force field and then, the properties were computed by single point calculation using the semi-empirical PM3 method. Based on the results (Table 17), the melanoidin structure proposed by Yaylayan and Kaminsky (1998) had the least value (most negative) of heat of formation (per water molecule). Thermodynamically, this is the most stable among the three proposed structures of melanoidin.

Table 17. Heat of Formation of Solvated Melanoidin

		Heat of Formation (kcal/ mol)	
Melanoidin structure	no. of H_2O	Solvated system	per water molecule
CK-[fructose-glycine]	207	-12221.405	-59.041
CK-[glucose-glycine]	206	-12194.125	-59.196
CK-[xylose-glycine]	200	-11635.019	-58.175
KT-[fructose-glycine]	207	-12028.417	-58.108
KT-[glucose-glycine]	207	-12083.589	-58.375
KT-[xylose-glycine]	210	-12166.102	-57.934
YK-[fructose-glycine]	205	-12112.476	-59.085
YK-[glucose-glycine]	204	-12136.859	-59.494
YK-[xylose-glycine]	210	-12299.503	-58.569

The heat of solvation can be defined as the change in enthalpy when a molecule is transferred from vacuum (or the gas phase) to a solvent. The solvation of a compound (A) can be represented as $A + nH_2O \rightarrow A \bullet nH_2O$ (Santos, 2003). HyperChem does not directly compute the heat of solvation. However, according to Lynden-Bell, et. al. (2001), the solvation energy can be computed as follows:

$$\Delta H_{sol} = \Delta H_{f,A \bullet nH_2O} - \left(\Delta H_{f,A} + \Delta H_{f,nH_2O}\right)$$

where: ΔH_{sol} = heat of solvation of A

$\Delta H_{f,A \bullet nH_2O}$ = heat of formation of $A \bullet nH_2O$

$\Delta H_{f,A}$ = heat of formation of A

$\Delta H_{f,nH_2O}$ = heat of formation of nH_2O

The heat of solvation of the three proposed structures of melanoidin were computed using the above equation (see Table 18).

Table 18. Computed Heat of Solvation of Melanoidin

Melanoidin	Heat of Formation (kcal/ mol) *in vacuo*	Solvated (no. of water)	Water only	Heat of Solvation (kcal/ mol)
C-K[fructose-glycine]	-872.060	-12221.405 (207)	-11337.091	-12.254
C-K[glucose-glycine]	-881.866	-12194.125 (206)	-11286.826	-25.433
C-K[xylose-glycine]	-718.376	-11635.019 (200)	-10928.312	-13.005
K-T[fructose-glycine]	-692.729	-12028.417 (207)	-11350.688	-69.779
K-T[glucose-glycine]	-770.660	-12083.589 (207)	-11347.700	—
K-T[xylose-glycine]	-623.737	-12166.102 (210)	-11515.772	-26.593
Y-K[fructose-glycine]	-942.279	-12112.476 (205)	-11249.860	—
Y-K[glucose-glycine]	-974.750	-12136.859 (204)	-11106.151	-55.958
Y-K[xylose-glycine]	-812.293	-12299.503 (210)	-11484.340	-2.870

The Yaylayan-Kaminsky (1998) structure of the glucose-glycine model system of melanoidin was used as model for ligand binding to the anionic exchange resin. HyperChem was used in docking melanoidin on the resin. Figure 20 shows the picture of melanoidin bound to a resin.

Figure 20. Melanoidin bound to anionic exchange resin

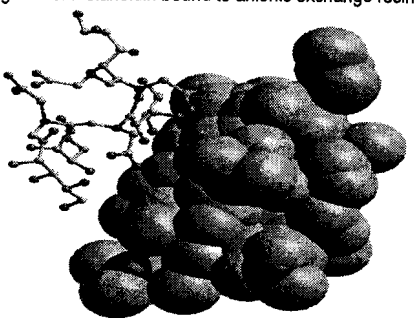

(a) melanoidin (ligand) and Amberlite IRA-410 (receptor)

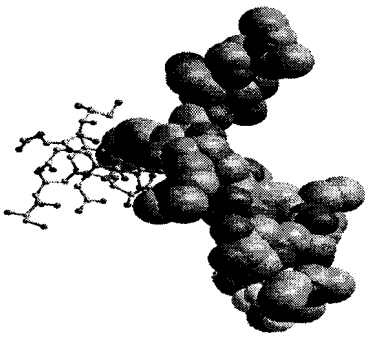

(b) melanoidin (ligand) and DEAE Sephadex (receptor)

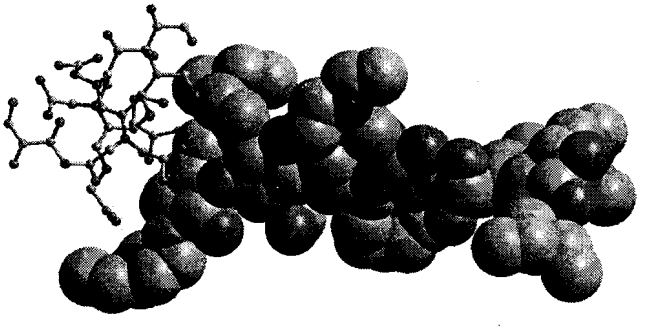

(c) melanoidin (ligand) and DEAE Cellulose (receptor)

Blind docking was also done using AUTODOCK software. From the computed values of the binding of the three anionic exchange resins, DEAE-Sephadex was observed to have the lowest E_{docked} and $\Delta G_{binding}$. Based on the experiental results, DEADE-Sephadex and DEAE-Cellulose have shown good performance in the decolorization of melanoidin. On the other hand, Amberlite IRA-410 docked with melanoidin but with positive value of $\Delta G_{binding.}$ This could be attributed to its weaker binding mode, which is due mostly to London dispersion interaction, compared to the other two complexes, which have a number of strong H-bonding interactions.

Summary and Conclusion

The melanoidin was decolorized using the anionic exchange chromatography method, ozonolysis and microbial method. All these methods showed the capability to decolorize melanoidin. Different types of synthetic adsorbent were tested in order to determine their capability to decolorize melanoidin. All the four commercial adsorbents tested (DOWEX 1-X8, Amberlite IRA-410, DEAE-Sephadex and DEAE-Cellulose), as well as chitosan (natural adsorbent), were able to decolorize the melanoidin sample. Among the five anionic exchangers examined, DEAE-Cellulose showed the best performance for melanoidin decolorization.

The actin of *Bacillus sp.* on the ozonated melanoidin showed significant changes in MW and MDA. However, for OZO-60 the melanoidin decolorization value fluctuated in the range 22-24% from day 1 to day 5. The UV-visible spectra of melanoidin showed considerable changes after ozonation and bacterial treatment. It can be concluded that ozonation and bacterial treatment are effective in decolorizing melanoidin.

From the computed heats of formation, it was observed that the structure proposed by Yaylayan and Kaminsky is the most probable mechanism for the formation of melanoidin.

Acknowledgement

Sincerest thanks

National Research Council of the Philippines

Source of Research Funds

Literature Cited

Amarante, J.A. 1998. Effect of pre-ozonation on decolorization and organic matter removal of distillery slops. Undergraduate thesis. UPLB.

Atkins, P.W. 1998. Physical Chemistry.

Baclay, O. P., Jr. 2002. "Molecular Orbital Calculations on the Maillard Reactions Involving Different Substrates. B.S. Chemistry Thesis. UPLB.

Billmeyer, F.W. Jr. 1984. 3rd ed. Textbook of Polymer Science. J. Wiley and Sons: N.Y, 208-213 pp.

Billingham, N. C. 1977. Molar Mass Measurements in Polymer Science. Wiley and Sons: New York, 172-185 pp.

Cämmerer, B. and L.W. Kroh. 1995. Investigation of the Influence of Reaction Conditions on the Elementary Composition of Melanoidins. *Food Chemistry.* 53: 55-59.

Carey, F.A. and R.J. Sunberg. 2001. 4th ed. Advance Inorganic Chemistry. Kluwer Academic/Plenum Publishers: Charlotte, Virginia, 788-790 pp.

Del Rosario, E.J. 1993. Chemical and Microbial Decolorization of Molasses- Derived Melanoidin. *Kimika.* 9: 65-72.

Escosia, T.M. 2001. Thermogravimetric and Spectroscopic Studies on the Solvent-Free Maillard Reaction (in melt) Between Glucose and Glycine. B.S. Chem Thesis. UPLB.

Fox, M.A. and J. Whitesell. 1997. Core Organic Chemistry. USA: Jones and Bartlett Publishers, Inc.

Hernandez, M. 2001. "Kinetic Studies on the Fructose-Glycine Maillard Reaction in Buffered Solution at pH 6, 7 and 8 (65°C)." BS Chemistry Thesis. UPLB.

Hudlicky, M. 1990. Oxidations in Organic Chemistry. Library of Congress Cataloging-in-Publication Data: United States of America.

HYPERCHEM. 1996. Computational Chemistry. Canada: Hypercube, Inc.

Jorgensen, W.L., Chandrasekhas, J., madura, J.D., Impey, R.W. ad M.L. Klein. 1983. Comparison of simple potential functions for silulation liquid water. *J. Chem. Phys.* 79:926-935.

Kato, H. and H. Tsuchida. 1981. Estimation Of Melanoidin Structure By Pyrolysis and Oxidation. Prog. Food And Nutri. Sci. 5:147-156.

Kim, S.B., Hayase F. and H. Kato. 1985. Decolorization and Degradation Products of Melanoidin on Ozonolysis. *Agric. Biol. Chem.* 49 (3):785-792.

Lynden-Bell, R.M., J.C. Rasaiah and J.P. Noworyta. 2001. Using simulation to study solvation in water. *Pure Applied Chem.* 73:1721-1731.

Macatangay, N.P. unpublished. Spectroscopic and Computational (UV-Vis and IR) Studies on reaction between ozone and Glucose-glycine melanoidin. B.S. Chem Thesis. UPLB.

McMurry, J. F. 1994. Organic Chemistry. Brooks/Cole Publishing.

Migo, V.P., del Rosario, E.J. and M. Matsumura. 1997. Flocculation of Melanoidins Induced by Inorganic Ions. *Ferment Bioeng.* 83:287-291.

Monterey, A.R. (2002). "Continuous-Flow Decolorization of Melanoidin-Containing Effluent Using an Anion-Exchange Column". B.S. Chemical Engineering Thesis. University of the Philippines at Los Baños.

Morrison and Boyd. 1992. Organic Chemistry 6th ed. New York: Prentice Hall. pp. 678-693.

Ohmomo, G., I. Aoshima, Y. Tozawa, N. Sakurada and K. Ueda. 1985. Purification and some properties of melanoidin decolorization enzymes, P 111 & P-IV, from mycelia of coriolus versicolor. Ps$a. *Agric. Biol. Chem.* 48(7):2047-2053.

O'Melia, C.R. In Ives, K. J. (ed.). 1978. The Scientific Basis of Flocculation. Sijthoff & Noordhoff, Alphen aan den Rijn, The Netherlands, 219-268 pp.

Rico, L.B. 1996. Changes in Some Molecular Properties of Synthetic and Natural Melanoidins After Decolorization by *Bacillus subtilis.* Undergraduate Thesis. UPLB.

Santos, A.K.S. 2003. Computational Studies on the Maillard Reaction of xylose and glycine/ butylamine in water. Undergraduate thesis. UPLB

Scopes, R. K. 1987. 2nd edition. Protein Purification. Sprinder-Verlag, 100-125 pp.

Sikales, N.M. and L. Segal (eds). 1971. 2nd ed. Cellulose and Cellulose Derivatives in High Polymers. Volume 5. Part 4. 469-486 pp.

Shriner, R.L., R.C. Fuson and D.Y.Curtin. 1998. 7th ed. The Systematic Identification of Organic Compounds: *A Laboratory Manual.* John Wiley and Sons, Inc: New York.

Wang, Y. 1990. Methanogenic Degradation Of Ozonation Products Of Biorefractory Of Toxic Aromatic Compounds. Water Res. 24(2): 185-190.

Weber, W. (ed). 1972. Physicochemical Processes For Water Quality Control. John Wiley And Sons, Inc.: New York. 363-411.

Whistler, R.L. and J.R. Daniel. In: Food Chemistry (Fennema, O.R., ed) 2nd ed. Carbohydrates, Marcel Dekker, N.Y. 96-104 pp.

Yaylayan, V. A. and Kaminsky. 1998. Isolation and Structural Analysis of Maillard Polymers: Caramel And Melanoidin Formation In Glycine-Glucose Model System. Food Chem. 63 (1):25-31.